2021

Sediment Nutrient Dynamics in Fondriest Agricultural Settling Pond

Marie Grace Bezold
Wright State University

SEDIMENT NUTRIENT DYNAMICS IN FONDRIEST AGRICULTURAL SETTLING POND

A thesis submitted in partial fulfillment of the
requirements for the degree of
Master of Science

by

MARIE GRACE BEZOLD

B.S., Northern Kentucky University, 2019

2021

Wright State University

WRIGHT STATE UNIVERSITY

GRADUATE SCHOOL

April 29, 2021

I HEREBY RECOMMEND THAT THE THESIS PREPARED UNDER MY SUPERVISION BY Marie Grace Bezold ENTITLED Sediment nutrient dynamics in Fondriest agricultural settling pond BE ACCEPTED IN PARTIAL FULFILLMENT OF THE REQUIREMENTS FOR THE DEGREE OF Master of Science.

_____

Silvia E. Newell, Ph.D.
Thesis Director

_____

Chad R. Hammerschmidt, Ph.D.
Interim Chair, Department of Earth and Environmental Sciences

Committee on Final Examination:

_____

Mark J. McCarthy, Ph.D.

_____

Rebecca E. Teed, Ph.D.

_____

Barry Milligan, Ph.D.
Vice Provost for Academic Affairs
Dean of the Graduate School

ABSTRACT

Bezold, Marie Grace. M.S., Department of Earth and Environmental Sciences, Wright State University, 2021. Sediment nutrient dynamics in Fondriest agricultural settling pond.

Excess loading of nitrogen (N) and phosphorus (P) is a serious global problem and has numerous negative impacts on water quality of aquatic ecosystems including eutrophication, harmful algal blooms, and hypoxia. Anthropogenic activities (such as the Haber-Bosch process, burning of fossil fuels, sewage treatment, and manure reuse) have led to excess N loading to aquatic systems. Sediment N dynamics were examined from Oct 2019 – Oct 2020 in an agricultural settling pond connected to a constructed wetland adjacent to an agricultural field. Intact sediment cores were amended with ^{15}N for continuous-flow incubations to measure denitrification and N fixation rates, as well as net nutrient and oxygen fluxes. Net N_2 consumption (N fixation > denitrification) was observed over most of the year, suggesting that pond sediments were a net N source. Denitrification was stimulated when ^{15}N-nitrate was added, and net denitrification was observed following a N fertilizer application in May 2020. NO_x entering the wetland and settling pond was rapidly transformed or assimilated. However, during winter and following fertilizer application, ambient NO_x concentrations increased in the wetland, but remained lower in the settling pond, suggesting rapid N removal in the pond. Sediment

oxygen demand and potential denitrification rates increased in warmer months, suggesting greater microbial activity and organic matter decomposition. Settling ponds in agricultural settings thus have the potential to supplement agricultural nutrient control practices. Further research should focus on understanding the frequency, timing, and amount of N loading that enters field-adjacent wetlands and ponds to determine if the sediments will consistently function as a net N sink and to maximize denitrification efficiency.

TABLE OF CONTENTS

Page

LIST OF FIGURES

LIST OF TABLES

ACKNOWLEDGEMENTS

I would first like to thank my advisors Dr. Silvia Newell and Dr. Mark McCarthy. I knew from our first meeting that you were who I wanted to work with and learn from over the next two years. You welcomed me immediately, constantly inspire me, push me, and always support me. I have learned and grown so much as a person and scientist because of the both of you. I cannot thank you both enough for the opportunities you offered me. You both have helped make my experience in graduate school so memorable and valuable, experiences I will always treasure and be able to build from.

I would also like to thank my third committee member Dr. Rebecca Teed for your constant support. It was a bit of a curveball switching to virtual teaching during the first semester I began TA'ing. This change was not as daunting as it could have been because I always felt you were an email or phone call away if I needed anything. You always made sure to check in with us during our weekly TA meetings and that means so much especially during these times.

I would also like to thank all my fantastic lab mates because you helped make my time in graduate school one to remember and were always there for me whether it be to celebrate an accomplishment, vent about life, or lend a helping hand. I want to give a special thank you to Kishan Gomez for braving the pond with me for most of (if not all) the samplings. Thank you to Justin Myers for teaching me so much about the MIMS, Lachat, field work, and all things in

between and happily answering my many questions. I often reflect back to when I first started in the lab getting flustered by anything that went wrong. Now I feel quite confident facing these same things and know so much more about the work that was at first so daunting to me because of all that you have taught me. I also want to specifically thank Joe Davidson, Lindsay Starr, Emily Holliday, Trevor Brannon, Shannon Collins, and Ian Crumrine because I could not have completed this research project without your help, smiles, encouragement, and support. Shannon and Ian, I will always treasure our friendship and the great times we have spent together.

I want to thank my boyfriend, Alex, who has been right by my side through my successes and struggles during grad school, I will always be grateful. I also want to thank my family who has always been so supportive of my endeavors. To my sister Elise, your passion for learning and teaching constantly inspires me. I also cannot forget to recognize my animals who I also consider my family and are such an important part of my life. Penelope, my (not so much anymore) puppy, I could not have imagined the happiness you have brought Alex and me (and the rest of the lab) when we adopted you two years ago. One of the greatest perks of spending so much time at home this past year has been your snuggles during the day when I am feeling extra stressed. To my horses, Buddy and Apollo, I could not imagine life without you. You have brought me so much joy and peace whether it be riding, reminiscing about our past accomplishments,

or spending time with you. I can forget all my worries while I am with you and that is something not many activities can offer, and the time spent with you is always a welcome break.

I. INTRODUCTION

Excess loading of nitrogen (N) and phosphorus (P) is a serious global problem and has numerous negative impacts on the water quality of lakes, rivers, and oceans (Smith et al., 1999), most notably eutrophication, defined as the proliferation of primary producers (Camargo and Alonso, 2006). Chlorophyll *a* concentration (a proxy for photosynthetic plankton biomass) greater than 20 µg/L is often considered the bloom threshold and leads to a decrease in water quality (Sutula et al., 2017). Hypoxia can subsequently result from high rates of decomposition of phytoplankton biomass and can affect invertebrates and fish. These effects reduce the recreational and land use value of the surrounding area, with losses estimated at $2.2 billion due to the negative impacts of eutrophication (Camargo & Alonso, 2006; Dodds et al., 2009; Wituszynski et al., 2017). Cyanobacteria often dominate the phytoplankton community in eutrophic lakes and can form harmful and potentially toxic blooms (Conley et al., 2009; Gupta et al., 2015). Cyanobacteria can be particularly detrimental because some species (e.g., *Microcystis aeruginosa*) can produce toxins, such as microcystin, which is a potent liver toxin and suspected tumor promoter (Wituszynski et al., 2017). Lake Erie is a notable example of a freshwater ecosystem that experiences large, seasonal cyanobacterial harmful algal blooms caused by excessive nutrient loading from fertilizer and waste runoff from an agricultural watershed (Chaffin et al., 2011). As a result of these blooms, the lake

experiences decreased water clarity, as well as development of bottom-water hypoxia in the central basin due to decomposition of phytoplankton biomass (Paerl & Otten, 2013; Wituszynski et al., 2017). Harmful algal blooms in Lake Erie caused a drinking water crisis in Toledo, Ohio in August 2014. The cyanobacterial bloom produced toxic microcystins which contaminated the water treatment system. The toxin concentration was measured at unsafe levels in the finished water (Steffen et al., 2017). This toxin incursion left more than 400,000 residents without tap water for 3 days, resulting in an estimated total cost of $65 million (Bingham et al., 2015). The Gulf of Mexico also experiences bottom-water hypoxia during summer months due to decomposition of phytoplankton blooms formed in surface waters. These blooms are fueled by excessive nitrate (NO_3^-) and P from fertilizer use in the agricultural watershed, which is discharged into the Mississippi River and, eventually, the Gulf of Mexico (Groh et al., 2015). These negative impacts from excessive nutrient loading exemplify the need to reduce N and P loading to the environment.

Anthropogenic activities (such as the invention and application of synthetic N fertilizers through the Haber-Bosch process, burning of fossil fuels, sewage treatment, and manure reuse as fertilizer) have led to excess N loading to aquatic systems. Between 1970 and 1990, anthropogenic activities doubled the rate of reactive N applied to the environment from 70 to 140 Tg N yr^{-1} (Galloway, 1998). This recent trend has caused N and P to be discharged in excess into the environment, allowing certain phytoplankton to outcompete others (e.g., non N_2 fixing cyanobacteria; Paerl, 2008). This significant increase in N use has a substantial impact on coastal and freshwater ecosystems and creates a need to manage N use and loads carefully (Hamilton et al., 2016; Smith et al.,

1999). One such approach for nutrient management is building edge-of-field constructed wetlands, as they can be an efficient and low-tech way to help filter nutrients.

Wetlands are a valuable, natural N mitigation resource and provide many other ecosystem services (e.g., habitats, flood control, sediment sinks; Morris et al., 1991). Wetlands can be efficient at reducing N loads because the range of redox conditions supports N transformation and removal pathways. These pathways include N retention or temporary removal through assimilation by macrophytes, phytoplankton, or microbes, or permanent loss through sediment burial or denitrification by facultative, anaerobic, heterotrophic bacteria (Burgin & Hamilton, 2007; Poe et al., 2003). Assimilation by plants produces biomass and only temporarily removes N from the system unless the vegetation is seasonally removed; otherwise, the N will become available again when plant organic matter is remineralized as ammonium (NH_4^+; Scott et al., 2008).

Denitrification is usually the dominant microbial N-loss pathway in freshwater systems and results in the removal of NO_3^- from the system as dinitrogen gas (N_2; Groh et al., 2015; Mulholland et al., 2008). Denitrification is the stepwise reduction of NO_3^- to nitrite (NO_2^-), to gaseous nitric oxide (NO), to gaseous nitrous oxide (N_2O), and, finally, to gaseous N_2, which is fully reduced and biologically unavailable, except to diazotrophs (Seitzinger et al., 1988; Poe et al., 2003). Nitrogen can also be transformed to N_2 gas through anaerobic ammonium oxidation (anammox), which occurs under anaerobic conditions and is performed by *Planctomycetes*, which are chemolithoautotrophic bacteria (Kuenen, 2008). In anammox, NH_4^+ is combined with NO_2^- to form N_2 gas, also resulting in permanent removal of N from the system. Anammox generally contributes minimally to total N_2 gas removal in freshwater systems, ranging between 0 and 30% of

total N_2 production (Boedecker et al., 2020; McCarthy et al., 2016; Schubert et al., 2006; Wenk et al., 2013).

Nitrate can alternatively be recycled through dissimilatory nitrate reduction to ammonium (DNRA). In the DNRA pathway, NO_3^- is reduced to NH_4^+, the most biologically available form of dissolved inorganic N. DNRA can be favored over denitrification under NO_3^- limited conditions that are rich in labile carbon, or in the presence of free sulfides (Burgin & Hamilton, 2007). Ammonium can then be assimilated by plants or microbes or be converted back to NO_3^- through nitrification, the aerobic oxidation of NH_4^+ to NO_3^- by chemoautotrophic bacteria (Vymazal, 2007), which completes the N cycle, as the NO_3^- can then be removed through coupled nitrification-denitrification (Jenkins & Kemp, 1984). Differing oxygen requirements for nitrification (aerobic conditions) and denitrification (anaerobic conditions) can uncouple these processes in hypoxic or anoxic stratified water or sediments.

New N can be added to the system through biological N fixation of N_2 gas into biomass, including by heterotrophic bacteria in sediments (Fulweiler et al., 2013; Galloway & Cowling, 2002; Herbert 1975; McCarthy et al., 2007). Factors influencing N fixation include N and P availability, the relative availability of N and P (N:P), temperature, and oxygen (O_2) concentrations (Howarth et al., 1988). Nitrogen fixation has been greatly altered by anthropogenic activities (Haber-Bosch), with an estimated 187 Tg of bioreactive N added yearly, a 320% increase in fixed N compared to preindustrial times (Vitousek et al., 2013). The N removal pathways supported by wetlands can result in high N removal efficiencies and help resolve the problem of excess N loading (Fisher & Acreman, 2004; Nichols, 1983). However, greater N loads decrease

N removal efficiency (Gardner & McCarthy, 2009; Mulholland et al., 2008). Unfortunately, a staggering percentage (87%) of natural wetlands have been destroyed by anthropogenic activities, and restoration of natural wetlands can be difficult, making constructed wetlands a desirable alternative (Clarkson et al., 2013; Davidson 2014).

Constructed wetlands are an attractive N mitigation approach because of their relatively low cost of construction, operation, and maintenance, and their creation has helped offset the impact of natural wetland losses (Gopal et al., 1999). Constructed wetlands are designed with the components that make up natural wetlands, such as vegetation and sediments with redox gradients, which allow them to effectively remove N (Vymazal et al., 2007). Thus, they can support the same permanent N removal pathways (e.g., denitrification, anammox) as natural wetlands (Gale et al., 1993; Poe et al., 2003; Scott et al., 2008). Constructed wetlands are effective at removing considerable proportions of the total N load applied to these systems (Lu et al., 2009; Mietto et al., 2015; Reinhardt et al., 2006). Denitrification can remove up to 94% of the total N in constructed wetlands, making these systems a valuable addition to areas receiving high N loads from agriculture (livestock, crop) operations and wastewater treatment plants (Reinhardt et al., 2006; Uusheimo et al., 2018a). Vegetation can temporarily remove N through assimilation into biomass, provide habitat for fauna and suitable conditions for microbe growth, and release O_2 from their roots, which can promote nitrification, an aerobic process, in an otherwise anaerobic milieu, thus supplying the substrate for denitrification (Kuschk et al., 2003; Lu et al., 2009; Reinhardt et al., 2006). The age of constructed wetlands is also an important factor in their ability to efficiently remove N, like their natural counterparts. It can take up to 10 years for constructed wetlands to

accumulate enough organic matter and establish the redox conditions needed to support high rates of denitrification (Craft, 1996; Nichols, 1983). Constructed wetlands can be effective N removal systems, but they may not be 100% efficient in N removal, suggesting that some combination of N removal systems, such as settling ponds associated with constructed wetlands, can help maximize nutrient removal.

Constructed wetlands in agricultural areas are often paired with settling ponds, which promote sedimentation of soil particles (Halide et al., 2003). Long retention times and low flow rates in settling ponds enhance sedimentation of suspended solids and improve water quality (Camargo Valero et al., 2010; Jackson et al., 2003; Teichert-Coddington et al., 1999). Sedimentation has previously been considered the dominant N removal process in wastewater stabilization ponds, a type of settling pond in a wastewater treatment setting (Ferrara and Avci, 1982; Senzia et al., 2002). Phytoplankton growth can be important to sedimentation and N removal, since these organisms assimilate N, then eventually may settle at the sediment surface after death (Camargo Valero et al., 2010). However, removal of N by sedimentation is only temporary as it could eventually be remineralized to NH_4^+. Thus, investigating the permanent N removal processes of denitrification and anammox in these types of ponds will offer valuable insight into the N cycle processes these systems can support.

The long retention time of settling ponds can offer a complex system for N transformations and removal to occur (Reed, 1985). More recent studies showed that wastewater stabilization pond systems can support denitrification (Camargo Valero et al., 2010; Keffala et al., 2011). Nitrogen transformations, including nitrification, mineralization, and assimilation have also been observed in these types of ponds (Mayo

& Abbas, 2014; Senzia et al., 2002). Wetlands alone may not remove the entire N load that enters the system, only removing up to 85% of N (Ilyas & Masih, 2017; Lee et al., 2009). Thus, by pairing constructed wetlands and settling ponds, nutrient removal can be maximized, since both systems can support N removal and transformation pathways. Healy and Cawley (2002) investigated a system comprising a free-water surface constructed wetland containing two reed bed cells and a retention pond cell, all connected in series. The study found that the entire system removed 64% of the total N, with the wetland cells removing a combined total of 51% and the retention pond removing 13% of total N. The retention pond was included in this system solely to increase retention time, but it also removed N, providing additional benefits. Thus, including settling ponds in a wetland system can increase the capacity for N transformation and removal pathways.

Wetlands are generally considered to be net N sinks (Jansson et al., 1994; Jordan et al., 2011; Scott et al., 2008), but the role of settling ponds in N removal is not well understood. Whether settling ponds function as a net N sink or source, and which N removal pathways and transformations are occurring in these ponds, remains uncertain. Most settling pond studies have focused on wastewater stabilization ponds, with little research on settling ponds that capture runoff from agricultural land. Recent studies showed that agriculture settling ponds are a net N sink, with up to 86% N removal efficiency (Powers et al., 2015; Tournebize et al., 2015; Zak et al., 2018). Agriculture ponds support denitrification, with rates dependent on N availability, temperature, seasonality, carbon supply, and rain events (David et al., 2006; Powers et al., 2015; Tournebize et al., 2015; Uusheimo et al., 2018b). However, other N cycle processes, such as nitrification, DNRA, remineralization, and anammox have not been thoroughly

investigated. The ratio of pond surface area to catchment size is important in determining denitrification rates (Bruesewitz et al., 2011; Uusheimo et al., 2018b). One study investigated agriculture drainage ditches and found that the overall N removal by denitrification was less than 1% due to the small surface area of the ditch systems compared to the size of the cultivated area (She et al., 2018). Even less settling pond research has involved combined wetland and settling pond systems in agricultural landscapes. Zak et al. (2018) investigated N removal in an integrated buffer zone, consisting of a ditch-like pond (surface flow) and a tree-planted, flow-through filter bed (subsurface flow), on the edge of an agriculture field. This study found that the system was a net N sink, with highest absolute N removal with increased N load, while N removal efficiency declined. Denitrification was not quantified specifically during this study, but anoxic conditions suggested that denitrification was active in the sediments. The combined or sequential use of settling ponds with wetlands as an edge-of-field mitigation strategy for reducing agriculture N loads is a relatively new study focus, with specific N cycle processes not evaluated thoroughly or at all. Thus, more research is needed to more fully understand the controls and the extent to which N transformations and removal pathways can be supported in combined wetland and settling pond systems located in an agriculture landscape.

The objectives of this project were to determine whether an agriculture settling pond—connected to a lateral, subsurface-flow, constructed wetland—acted as a net N source or sink and to determine which N transformation and removal pathways were active in pond sediments. The results from this study will help evaluate whether the role of settling ponds is beneficial beyond that of constructed wetlands draining agricultural

land. It was hypothesized that: (1) denitrification is the major removal pathway for NO_3^- in pond sediments; (2) pond sediments are a net N sink because of their proximity to an active agriculture field, providing N loads to the settling pond; (3) sediment net N_2 fluxes vary seasonally, with net denitrification dominating in spring through summer, then switching to net N fixation in fall through winter; and (4) sediments will be a source of NH_4^+ and soluble reactive P (SRP).

II. METHODS

Site Description

Water samples and sediment cores were collected from a constructed settling pond at the Fondriest Center for Environmental Studies in Fairborn, Ohio. The settling pond is connected to a lateral, subsurface flow constructed wetland; water entering the wetland passively overflows into the pond (Figure 1). There is no pumping or flow gauge within the wetland, so the flow rate and residence time are entirely dependent on local rainfall. The wetland is approximately 20 m in length, 6 m in width, and 1 m in depth. The wetland contains layers of rock decreasing in diameter: the bottom layer (0.3 m) contains river rock 7.6 cm in diameter, followed by 3.5 cm river rock, with pea gravel as the top layer. The settling pond is approximately 4,047 m^2, and the bank is lined with *Juncus effusus*. Various recreational fish species (e.g., bass and bluegill) were also stocked into the pond. The location is adjacent to an agricultural farm field (~30,000 m^2; corn or soybean row crop; Figure 2). Surface runoff, including any mobile proportion of fertilizer applied throughout the year, is discharged into adjacent, natural wetlands and the constructed wetland, as well as, during heavy precipitation events, directly into the settling pond.

Fertilizer Application

Nitrogen-containing fertilizer was applied to the 30,000 m^2 crop field during 2019 and 2020 (Table 1). 28-0-0 fertilizer, containing 28% N of the total weight, was applied

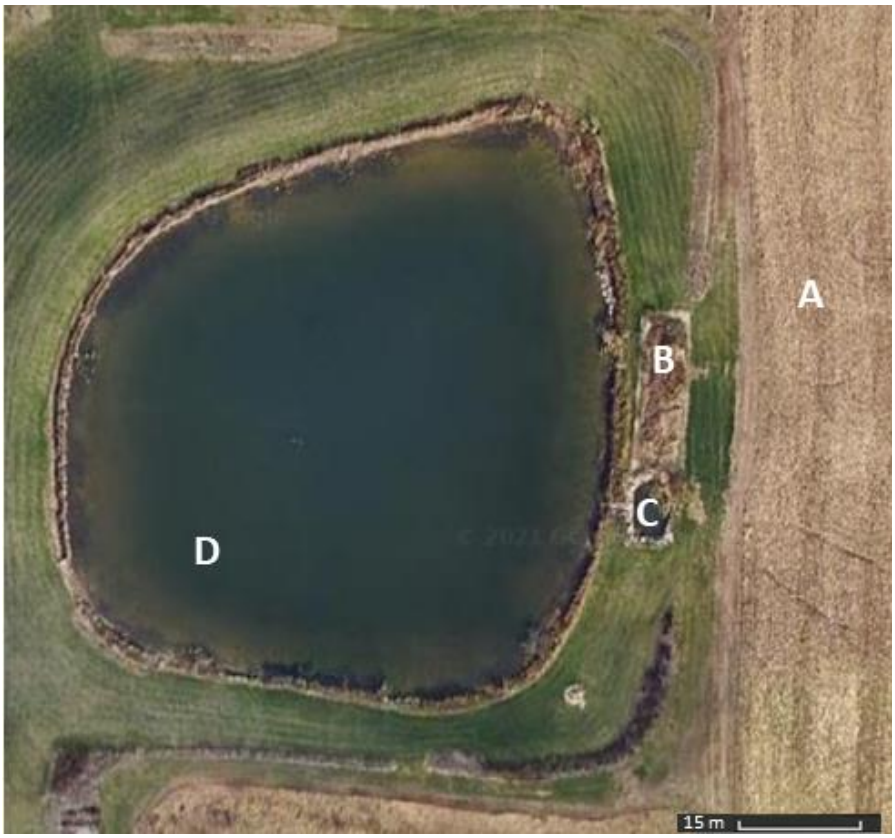

Figure 1. Aerial view of sampling site including the (A) agricultural farm field, (B) wetland inlet, (C) wetland outlet, and (D) sample collection site within the constructed wetland. Image retrieved from Google Maps.

Figure 2. Aerial view of sampling site and surrounding area including the (A) agricultural farm field, (B) wetland, and (C) settling pond. Image retrieved from Google Maps.

Table 1. Date of fertilizer applications, total nitrogen (N) applied, and type of fertilizer applied to the crop field adjacent to the settling pond between June 2019 and May 2020. NPK: Nitrogen-Phosphorus-Potassium.

Date	Total N (L)	Fertilizer (NPK)
6/4/2019	152	28-0-0
7/15/2019	207	28-0-0
5/22/2020	8.3	6-24-6

on June 4, 2019, and July 15, 2019. 28-0-0 fertilizer generically contains 6.9% urea, 6.9% NH_4^+, and 14.2% NO_3^- (https://www.nutrien.com/sites/default/files/products/datasheet/POT_SS_FER_URAN28.pdf). 6-24-6 fertilizer, generically containing 6% N (as NH_4^+), 24% P, and 6% potassium (https://www.cropchoicefertilizer.com/wp-content/uploads/2018/07/CropChoice-6-24-6-and-6-24-6-1S.pdf), was applied on May 22, 2020.

Sample Collection

Nine intact sediment cores with overlying water were collected from the western side of the settling pond using a coring device designed to preserve redox gradients in the sediment core and overlying water (Figure 3; Gardner and McCarthy, 2009). Cores were collected approximately monthly between September 2019 and October 2020. Four, 20 L Cubitainers (two for unamended controls, one for $^{15}NO_3^-$ amendments, and one for $^{15}NH_4^+$ amendments) were filled with pond water to be used as inflow reservoirs for continuous-flow incubations. The second unamended Cubitainer was reserved for topping off treatment inflow reservoirs to ensure that enough site water was available to supply the triplicate cores for the duration of the incubations.

Water samples for ambient nutrient analyses were collected from the settling pond during each sampling event. These samples were filtered with a clean, 60 mL syringe and 0.22 µm Nylon syringe filter (Millipore) after rinsing with at least 5 mL of site water. Water samples for nutrient analyses were collected in 15 mL polypropylene tubes for SRP, NH_4^+, NO_2^-, NO_3^-, and urea analyses. The tubes were stored frozen until analysis. Physicochemical parameters, including water temperature, depth, pH, specific

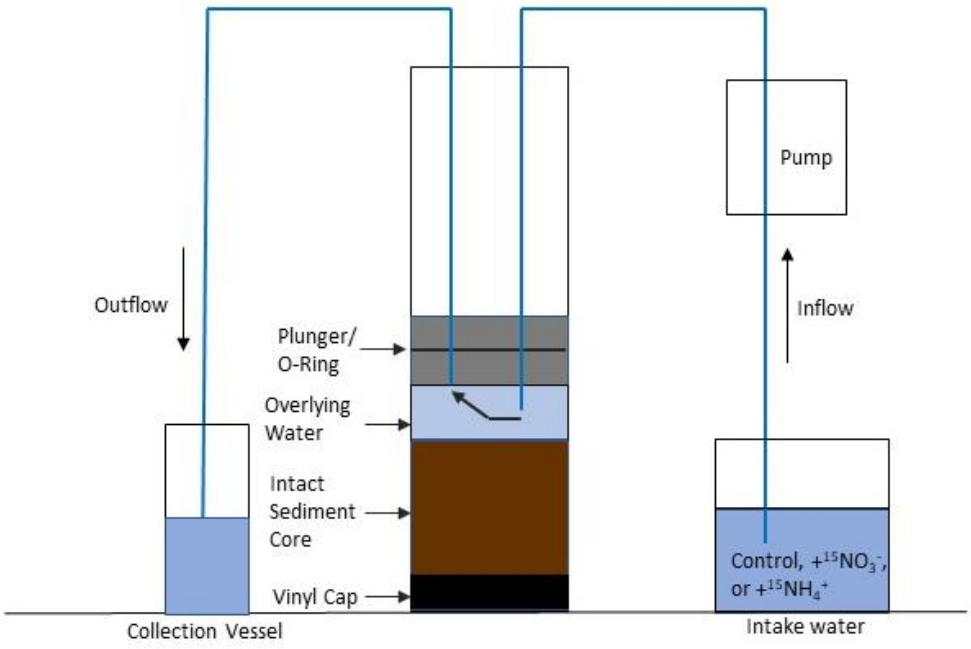

Figure 3. Diagram of the continuous flow incubation system using intact sediment cores (modified from Lavrentyev et al., 2000).

conductivity, chlorophyll *a* fluorescence, blue-green algae cells, and dissolved oxygen (DO) concentration, were measured at the surface and near-bottom of the pond using a Eureka Manta 2 Sonde at the time of sampling.

Sediment Core Incubations

All sediment core incubations were conducted in the lab at Wright State University (WSU), except for those that occurred in May and July 2020 (5/6/20, 5/26/20, 7/1/20, 7/28/20). The May and July 2020 incubations occurred in an open-air lab due to COVID-19 shutdown of the WSU campus, with an added benefit of allowing incubation temperatures to better represent *in situ* temperature. The WSU lab was kept at a constant 18°C, while the air temperature during the spring and summer months ranged from 26°C to 32°C.

Continuous-flow sediment core incubations were used to measure N removal and recycling, in addition to net nutrient and oxygen fluxes (Lavrentyev et al., 2000; McCarthy et al., 2015). Three treatments were initiated with triplicate cores: (1) unamended control (C; no amendment); (2) $^{15}NH_4^+$ amended (A; used to quantify possible anammox), and (3) $^{15}NO_3^-$ amended (N; used to calculate N fixation and quantify potential denitrification and DNRA rates). The C cores were used to measure the net $^{28}N_2$, O_2, and nutrient fluxes (SRP, NH_4^+, NO_2^-, NO_3^-, and urea). The $^{15}NH_4^+$ amendment (A cores) was used to measure possible anammox rates by following the added $^{15}NH_4^+$ isotopic tracer, which could be combined with *in situ* $^{14}NO_2^-$ to produce $^{29}N_2$. $^{29}N_2$ production is considered possible anammox because $^{29}N_2$ could also be produced through coupled nitrification-denitrification (i.e., $^{15}NH_4^+$ nitrified to $^{15}NO_3^-$ and combined with ambient $^{14}NO_3^-$ to produce $^{29}N_2$ via denitrification; McCarthy et al.,

2015). The A treatment was spiked to ~5 µM final concentration in the inflow reservoir using 10 mM $^{15}NH_4Cl$ stock solution. The $^{15}NO_3^-$ amendment (N cores) was used to measure potential denitrification and DNRA rates and calculate N fixation using the reduction of NO_3^- to $^{28}N_2$ ($^{14}NO_3^-$), $^{29}N_2$ ($^{14}NO_3^-$ and $^{15}NO_3^-$), or $^{30}N_2$ ($^{15}NO_3^-$; An et al., 2001). The N treatment was spiked to ~50 µM NO_3^- final concentration using 50 mM $Na^{15}NO_3$ stock. Dissolved O_2 and isotopic N_2 produced from all three treatments were quantified using a membrane inlet mass spectrometer (MIMS; An et al., 2001, Kana et al. 1994).

Intact sediment cores were prepared for incubation by carefully siphoning the overlying water from the cores until approximately 5 cm of water remained above the sediment surface. An air- and water-tight Delrin plunger fitted with an O-ring and gas-tight inflow and outflow polyetherketone (PEEK) tubing was inserted into each core tube until the inflow tubing was approximately 1 cm above the sediment surface (Figure 3). Each sediment core was wrapped with aluminum foil to prevent any light effects. Two peristaltic pumps (Rainin Dynamax®) were used to supply the sediment cores with a constant supply of overlying water at a flow rate of approximately 1.5 mL min^{-1}.

Intact sediment cores were pre-incubated for ~24 hours to allow establishment of equilibrium conditions. Triplicate inflow and outflow dissolved gas and nutrient samples were collected daily for three days. Water samples were collected near-simultaneously from core inflows and outflows for dissolved nutrient (SRP, NH_4^+, NO_2^-, NO_3^-, and urea) and OxMIMS ($^{15}NH_4^+$; Yin et al., 2014) analysis. Nutrient samples were immediately filtered using a 0.22 µm Nylon syringe filter, and four 15 mL polypropylene tubes and one 12 mL exetainer (no headspace) were filled for dissolved nutrient and OxMIMS

analyses, respectively. Nutrient samples were stored frozen at -20ºC until analysis on the Lachat QuikChem© 8500 Flow Injection Analysis System at Wright State University. Exetainers were stored in the dark at room temperature until analysis using the OxMIMS method (Yin et al., 2014). OxMIMS measures dissolved $^{15}NH_4^+$ concentrations by using a BrO^- iodine solution to oxidize dissolved NH_4^+ to N_2, which can then be measured with MIMS to quantify DNRA (as $^{15}NH_4^+$ produced from $^{15}NO_3^-$).

Dissolved gas concentrations (O_2, $^{28}N_2$, $^{29}N_2$, $^{30}N_2$) were measured on the MIMS immediately when incubated in the WSU lab or preserved and analyzed within two weeks when incubated in the open-air lab. Dissolved gas samples were collected directly from each inflow and outflow. Inflow samples were collected using a syringe to fill a 15 mL tall glass tube (Chemglass) designed to minimize surface-to-volume ratio. Outflow samples were collected by allowing the 15 mL glass tubes to overflow with sample water. During the four incubations that occurred in the open-air lab, dissolved gas samples were collected in Exetainers, allowed to overflow, preserved with 200 µL of 50% (w/w) $ZnCl_2$ to stop microbial activity, capped, and stored in the dark at room temperature until analysis.

Dissolved Nutrient Analysis

Ambient water column and sediment core samples were analyzed for nutrients (SRP, NO_x, NH_4^+, and urea) using the Lachat QuikChem© 8500 Flow Injection Analysis System at Wright State University according to manufacturer's instructions. Reagents used for each method react with the sample to create a colored product to be measured at the appropriate absorbance for the method. A standard curve was generated for each

analyte using known concentration standards and used to calculate unknown concentrations in samples.

SRP (QuikChem© Method 31-115-01-1-I) was analyzed using a molybdate color reagent made from NH_4^+ molybdate and antimony potassium tartrate stock solutions, ascorbic acid reducing solution, and NaOH with an EDTA rinse, used at the end of each run to rinse the transmission tubing lines. The absorbance used in this method was 880 nm, and the determined minimum detection limit (MDL) was 0.011 µM, which was lower than the manufacturer's stated MDL (0.03 µM). Calibration standards were prepared using K_3PO_4 (10, 5, 2, 1, 0.5, 0.1, 0.03, and 0 µM), with a 3.22 µM quality control sample (QCS).

Ammonium (QuikChem© Method 31-107-06-1-G) was analyzed using sodium phenolate, sodium dichloroisocyanurate (DCIC), and sodium nitroprusside/Na_4EDTA buffer solution. The absorbance used in this method was 630 nm, and the determined MDL was 0.20 µM. Calibration standards were made using NH_4Cl (25, 10, 5, 2.5, 1.5, 0.75, 0.25, 0.10, and 0 µM), with a 7.14 µM QCS.

Nitrate and NO_2^- (QuikChem© Method 31-107-04-1-E) were analyzed using two channels simultaneously. One channel measured NO_2^- only, and the other channel measured $NO_3^- + NO_2^-$, which was determined by reducing NO_3^- to NO_2^- using a Cd column. Both methods used an NH_4Cl buffer (pH = 8.5) and sulfanilamide color reagent to react with NO_2^-. The absorbance used in this method was 540 nm, and the determined MDL was 0.036 µM. Calibration standards were prepared using $NaNO_2$ (40, 20, 10, 5, 1, 0.5, 0.25, 0.10, and 0 µM), with a 20 µM NO_3^- QCS.

Urea (QuikChem© Method 31-206-00-1-A) was analyzed using an acid reagent (containing H_2SO_4, H_3PO_4, and $FeCl_3$), a color reagent (containing diacetyl monoxime solution and thiosemicarbazide solution), and a carrier rinse (0.84 M NaCl). The determined MDL was 0.21 µM. Calibration standards were made using urea (20, 10, 5, 2.5, 1, 0.75, 0.37, and 0 µM).

Data Calculations and Statistics

Dissolved gas and nutrient fluxes were calculated from each of the three treatments using the following equation:

$$Flux = (C_o - C_i) \; x \; f \; / \; a$$

Where C_o is the concentration in the outflow, C_i is the concentration in the inflow, f is the flow rate, and a is the sediment core surface area (0.0045 m^2; Lavrentyev et al., 2000; McCarthy et al., 2015). Net $^{28}N_2$ flux was determined from the C cores and represented the balance of simultaneous denitrification and N fixation. A positive flux indicated a net efflux of $^{28}N_2$ out of the sediment, where the rate of N fixation was lower than combined denitrification and anammox. A negative flux indicated an influx of $^{28}N_2$ into the sediment, where the rates of denitrification and anammox were lower than N fixation. The sum of $^{28,29,30}N_2$ and any calculated N fixation from the N cores was considered potential denitrification, and net $^{28}N_2$ flux in C cores plus any calculated N fixation from N cores represented the best estimate of *in situ* denitrification. Any $^{29}N_2$ production from the A cores represented possible anammox. Calculated N fixation was determined from the N cores using a quadratic equation (An et al., 2001).

Daily precipitation data was compiled from the Xenia weather station, located ~11 km from the sampling site, on Weather Underground (https://www.wunderground.com/history). Statistics were performed in JMP using nonparametric tests because the data were not normally distributed. Normality was determined using the Anderson Darling normality test. Comparisons between treatments were performed using the Wilcoxon Signed-Rank test, while the Kendall's tau (τ) correlation was used for a measure of similarity. Graphs were constructed using Microsoft Excel 2016.

III. RESULTS

Wetland and Pond Monitoring Data

Ambient NO_2^-, NO_3^-, urea, and SRP samples were collected approximately monthly from the wetland inlet and outlet and settling pond between February 22, 2019, and September 1, 2020. The inlet represented overland flow into the wetland, and the outlet represented direct outflow from the wetland into the settling pond. During winter and following fertilizer applications, the wetland was a source of NO_3^-, with higher concentrations observed in the outlet versus the inlet (Wilcoxon Signed-Rank; $p < 0.05$), while concentrations of both NO_2^- (Wilcoxon Signed-Rank, $p < 0.05$) and NO_3^- (Wilcoxon Signed-Rank, $p < 0.05$) remained lower in the settling pond compared to the outlet (Table 2). Ambient NO_2^- concentrations ranged from 0.070 to 5.99 µM (median = 0.183 µM) and from below detection limit (BDL) to 56.4 µM (median = 0.323 µM) in the inlet and outlet, respectively. Ambient NO_3^- concentrations ranged from BDL to 181 µM (median = 1.28 µM) and BDL to 438 µM (median = 4.64 µM) in the inlet and outlet, respectively. Ambient NO_2^- (range: BDL to 0.529µM) and NO_3^- (range: BDL to 15.7 µM) concentrations were generally lowest in the settling pond (Table 2). Ambient NO_x concentrations were higher in the wetland during the winter compared to concentrations during the rest of the year, except on June 7, 2019, which followed an N fertilizer application three days prior (Table 1). Ambient NO_2^- and NO_3^- concentrations consistently remained lower in the settling pond

Table 2. Ambient oxidized nitrogen concentration data collected during monthly monitoring from February 2019 to September 2020 from the wetland inlet and outlet and the settling pond. Units are µM N. Samples below detection limits are reported as less than that method's limit. Monitoring dates do not always align with sampling dates. ND = no data.

Sampling Date	NO_2^-			NO_3^-		
	Inlet	Outlet	Pond	Inlet	Outlet	Pond
2/22/2019	0.183	0.476	0.240	157	182	15.7
3/27/2019	0.680	0.864	0.529	13.2	42.30	7.14
5/9/2019	0.157	<0.036	0.098	1.28	0.556	0.533
6/7/2019	5.99	56.4	0.251	181	438	4.18
7/11/2019	0.120	0.816	<0.036	1.24	7.80	0.118
8/16/2019	0.140	<0.036	<0.036	<0.036	<0.036	<0.036
9/30/2019	0.166	0.060	<0.036	0.918	<0.036	<0.036
10/25/2019	0.282	0.090	<0.036	<0.036	0.040	0.040
11/27/2019	0.333	0.170	<0.036	36.4	10.1	0.739
1/27/2019*	0.236	0.691	<0.036	30.0	45.6	1.18
2/26/2020	0.696	1.07	<0.036	43.7	68.3	0.057
5/10/2020	0.093	0.150	<0.036	0.123	1.47	0.046
8/1/2020	ND	0.047	<0.036	ND	0.151	0.079
9/1/2020*	0.070	3.22	<0.036	<0.036	1.16	0.086
Mean (±SE)	0.703 (0.444)	4.57 (3.99)	0.088 (0.041)	35.8 (17.0)	56.9 (32.1)	2.14 (1.18)

*Monitoring and sampling occurred on same date.

than in the wetland at all sampling events.

Ambient urea concentrations were not different between the wetland inlet (range: 0.705 to 2.64 µM) and outlet (range: 0.973 to 4.015 µM; Table 3). However, ambient urea concentrations in the settling pond were lower than those in both the inlet (Wilcoxon Signed-Rank, $p < 0.05$) and outlet (Wilcoxon Signed-Rank, $p < 0.05$).

Ambient SRP concentrations remained below 0.9 µM in the wetland inlet (mean: 0.446 ± 0.082 µM), outlet (mean: 0.142 ± 0.041 µM), and settling pond (mean: 0.045 ± 0.007) at all sampling events (Table 4). Inlet SRP concentrations were higher than both the outlet (Wilcoxon Signed-Rank, $p < 0.05$) and settling pond (Wilcoxon Signed-Rank, $p < 0.05$). Ambient SRP concentrations were also higher in the outlet compared to the settling pond (Wilcoxon Signed-Rank, $p < 0.05$).

Ambient Environmental Patterns

Surface and bottom water temperatures of the settling pond followed expected seasonal patterns, with warmer temperatures during the spring and summer and cooler temperatures during the fall and winter (Tables 5 and 6). Generally, surface water temperature was higher than bottom water temperature. Both surface and bottom water temperatures peaked on July 1, 2020, to 29.8°C and 28.9°C, respectively. Likewise, the coldest surface and bottom water temperatures were observed on January 27, 2020, when the settling pond was ice covered, at 4.13°C and 3.79°C, respectively. Surface and bottom water pH ranged from 7.50 to 8.75 throughout all sampling events. pH was similar in the bottom water (mean = 8.19 ± 0.07) and surface water (mean = 8.14 ± 0.09).

Table 3. Ambient urea concentration data collected during monthly monitoring from October 2019 to December 2020 from the wetland inlet and outlet and the settling pond. Units are μM N. Samples below detection limits are reported as less than that method's limit. Monitoring dates do not always align with sampling dates. ND = no data.

Sampling Date	Inlet	Outlet	Pond
10/25/2019	2.059	1.331	1.401
11/27/2019	1.629	0.973	0.689
1/27/2019*	1.548	1.164	0.840
2/26/2020	2.641	2.549	0.380
5/10/2020	2.307	1.916	0.807
8/1/2020	0.705	2.067	0.701
9/1/2020*	ND	4.015	ND
Mean (±SE)	1.698 (0.263)	1.937 (0.349)	0.802 (0.116)

*Monitoring and sampling occurred on same date.

Table 4. Ambient soluble reactive phosphorus (SRP) concentration data collected during monthly monitoring from March 2019 to December 2020 from the wetland inlet and outlet and the settling pond. Units are µM P. Samples below detection limits are reported as less than that method's limit. Monitoring dates do not always align with sampling dates. ND = no data.

Sampling Date	Inlet	Outlet	Pond
3/27/2019	0.215	0.063	0.073
5/9/2019	0.417	0.036	0.032
9/30/2019	0.752	0.049	0.012
10/25/2019	0.860	0.086	0.048
11/27/2019	0.099	0.460	0.045
1/27/2019*	0.292	0.079	0.050
2/26/2020	0.235	0.091	0.038
5/10/2020	0.740	ND	0.026
8/1/2020	ND	0.141	0.039
9/1/2020*	0.393	0.135	ND
Mean (±SE)	0.446 (0.082)	0.142 (0.041)	0.045 (0.007)

*Monitoring and sampling occurred on same date.

Table 5. Surface water (depth ≤ 0.10 m) physicochemical data collected during sediment sampling events between September 30, 2019, and October 6, 2020. ND = no data. Temp = Temperature, Sp Cond = Specific Conductance, Chl *a* = Chlorophyll *a*, BG = Blue-green algae cells, DO = Dissolved Oxygen.

Sampling Date	Temp (°C)	pH	Sp Cond (µS cm^{-1})	Chl *a* (µg L^{-1})	BG Cells (mL^{-1})	DO (mg L^{-1})
9/30/19	27.0	8.17	184	17.7	0.82	7.74
10/29/19	ND	ND	ND	ND	ND	ND
12/2/19	5.65	8.15	186	13.0	0.25	12.1
1/27/20	4.13	8.25	188	4.68	0.45	13.8
3/9/20	7.65	7.68	182	8.20	1.22	11.7
5/6/20	15.4	8.14	176	ND	ND	9.55
5/26/20	28.1	7.71	178	4.11	0.70	8.38
7/1/20	29.8	8.22	202	ND	ND	7.37
7/28/20	ND	8.14	195	5.80	2.00	7.60
9/1/20	26.3	8.29	188	4.54	0.75	7.52
10/6/20	16.0	8.65	185	1.57	0.31	9.20

Table 6. Bottom water physicochemical data collected during sediment sampling events between September 30, 2019, and October 6, 2020. ND = no data. Temp = Temperature, Sp Cond = Specific Conductance, Chl *a* = Chlorophyll *a*, BG = Blue-green algae cells, DO = Dissolved Oxygen.

Sampling Date	Depth (m)	Temp (°C)	pH	Sp Cond ($\mu S\ cm^{-1}$)	Chl *a* ($\mu g\ L^{-1}$)	BG Cells (mL^{-1})	DO ($mg\ L^{-1}$)
9/30/19	1.65	23.7	7.76	186	35.7	1.84	4.85
10/29/19	1.45	14.0	8.47	184	26.5	0.99	10.6
12/2/19	0.38	5.66	8.2	186	12.8	0.5	12.0
1/27/20	0.67	3.79	8.33	184	9.21	3.20	14.0
3/9/20	0.53	7.56	8.03	182	14.8	1.98	12.2
5/6/20	0.88	15.0	8.21	176	5.93	3.19	9.68
5/26/20	0.6	24.2	7.98	178	8.49	2.00	8.84
7/1/20	0.74	28.9	8.11	201	2.85	1.47	7.48
7/28/20	0.78	ND	8.17	195	6.75	1.43	6.91
9/1/20	0.75	26.2	8.24	188	8.50	1.26	7.29
10/6/20	0.66	15.9	8.63	185	2.76	2.1	10.1

Chlorophyll *a* concentrations were generally higher in the bottom water (mean = 12.2 ± 3.09 µg L^{-1}) than in the surface water (mean = 5.93 ± 1.80 µg L^{-1}). Surface and bottom water DO concentrations were not different, although, bottom water DO was generally higher than surface water DO. Dissolved oxygen also followed an expected seasonal trend, with higher concentrations in the winter. Surface water DO was negatively correlated with surface water temperature (τ = -0.83, p = 0.0018; Table 7), and, likewise, total daily precipitation was variable throughout the sampling period, ranging from 0 to 5.8 cm (Figure 4). Total precipitation was greatest during the spring 2020 season (mean = 0.76 ± 0.16 cm). Mean precipitation was successively lower in winter 2019/2020 (mean = 0.67 ± 0.12 cm), fall 2019 (mean = 0.58 ± 0.10), and summer 2020 (mean = 0.52 ± 0.09 cm).

Ambient nutrients (SRP, NH_4^+, NO_3^-, NO_2^-, and urea) were collected from the settling pond at each sampling event (Table 8). SRP concentrations ranged from 0.012 to 0.051 µM throughout all sampling events (median = 0.037 µM). Ammonium concentrations remained below 1.0 µM on all but three sampling events, ambient NH_4^+ results were BDL. On October 29, 2019, NH_4^+ increased to 2.56 µM. NH_4^+ concentration doubled to 5.34 µM on the next sampling event (December 2, 2019) and did not rise above 1.0 µM again until July 1, 2020 (3.81 µM). Nitrite concentrations were lower than NO_3^- concentrations (Wilcoxon Signed-Rank, $p > 0.05$) during all sampling events and remained below 0.16 µM (median = 0.014 µM). Ambient NO_2^- was positively correlated with NH_4^+ flux in C cores (τ = 0.48, p = 0.046; Table 7) and with DNRA (τ = 0.51, p = 0.04; Table 7). NO_3^- concentrations ranged from 0.05 to 1.95 µM (median = 0.209 µM). The highest NO_3^- concentration (1.947 µM) was observed on January 27, 2020. Ambient

Table 7. Kendall's tau (τ) correlation tests comparing sediment O_2 demand (SOD), net $^{28}N_2$ flux, net $^{29}N_2$ flux, *in situ* denitrification (DNF), DNF potential, nitrogen fixation (N fix), percent (%) anammox, dissimilatory NO_3^- reduction to NH_4^+ (DNRA), SRP flux, NH_4^+ flux, NO_2^- flux, NO_3^- flux, ambient (amb) SRP, amb NH_4^+, amb NO_2^-, amb NO_3^-, amb urea, surface (surf) temperature (temp), surf specific (sp) conductivity (cond), surf chlorophyll *a* (chl *a*), surf blue-green (BG) cells, surf dissolved oxygen (DO), bottom (bot) temp, bot pH, bot sp cond, bot chl *a*, bot BG cells, and bot DO. C = control (unamended) cores, A = $^{15}NH_4^+$ amended cores, ND = no data.

	C SOD	C Net $^{29}N_2$	A Net $^{29}N_2$	*In Situ* DNF	DNF Pot	N Fix	% Anammox	DNRA	C PO4 Flux	C NH4 Flux	C NO2 Flux	C NO3 Flux	C Urea Flux	Amb PO4	Amb NH4	Amb NO2	Amb NO3	Amb Urea	Surf Temp (°C)	Surf pH	Surf Sp Cond (µS cm-1)	Surf Chl a (µg L-1)	Surf BG Cells (mL-1)	Surf DO (mg L-1)	Bot Temp (°C)	Bot pH	Bot Sp Cond (µS cm-1)	Bot Chl a (µg L-1)	Bot BG Cells (mL-1)	Bot DO (mg L-1)
C SOD	1.00																													
C Net $^{29}N_2$	0.02	1.00																												
A Net $^{29}N_2$	0.35	0.27	1.00																											
***In Situ* DNF**	0.09	0.20	0.16	1.00																										
DNF Pot	**0.56**	0.16	0.35	0.09	1.00																									
N Fix	-0.02	**-0.63**	-0.09	0.02	-0.24	1.00																								
% Anammox	0.16	0.20	**0.82**	0.13	0.16	0.09	1.00																							
DNRA	0.37	-0.25	-0.14	0.10	0.17	-0.02	-0.25	1.00																						
C SRP Flux	0.16	-0.02	0.45	0.05	-0.06	0.16	**0.56**	-0.02	1.00																					
C NH_4^+ Flux	0.42	-0.13	0.20	0.24	0.05	0.05	0.16	**0.60**	0.24	1.00																				
C NO_2^- Flux	0.20	0.31	**0.49**	0.31	0.20	-0.09	0.45	0.10	0.16	0.27	1.00																			
C NO_3^- Flux	0.45	**0.56**	0.45	0.13	**0.60**	**-0.49**	0.27	-0.06	0.05	0.09	0.38	1.00																		
C Urea Flux	0.31	0.13	0.31	0.13	0.02	-0.06	0.35	-0.10	0.27	0.24	0.24	0.27	1.00																	
Amb SRP	0.18	**-0.47**	-0.15	-0.29	0.07	0.33	-0.18	0.43	0.18	0.26	-0.11	-0.26	-0.22	1.00																
Amb NH_4^+	-0.34	0.30	0.26	ND	-0.13	-0.04	0.21	-0.20	-0.04	-0.13	0.43	0.00	-0.09	-0.19	1.00															
Amb NO_2^-	0.21	-0.09	0.21	ND	0.02	0.17	0.17	**0.51**	0.10	**0.48**	0.44	-0.13	-0.21	0.25	0.34	1.00														
Amb NO_3^-	-0.34	-0.16	-0.13	0.05	-0.06	0.09	-0.09	0.13	-0.31	0.02	0.09	-0.24	**-0.53**	0.07	0.26	0.40	1.00													
Amb Urea	0.20	0.24	0.05	**0.67**	0.27	-0.09	-0.06	0.25	-0.27	0.20	0.42	0.31	0.02	-0.18	-0.04	0.06	0.09	1.00												
Surf Temp (°C)	**0.61**	0.44	0.22	0.06	**0.89**	**-0.56**	0.06	0.20	-0.22	0.06	0.06	**0.72**	0.06	-0.08	-0.07	-0.03	-0.22	0.33	1.00											
Surf pH	-0.27	-0.22	-0.32	**-0.54**	-0.09	0.04	-0.23	0.07	-0.13	-0.27	-0.27	-0.22	**-0.67**	0.39	0.14	0.17	0.31	-0.27	0.00	1.00										
Surf Sp Cond (µS cm^{-1})	-0.11	0.20	0.11	-0.16	0.24	-0.24	-0.07	-0.28	0.02	-0.24	-0.02	0.20	-0.24	-0.18	0.33	0.07	0.24	-0.16	0.17	0.22	1.00									
Surface Chl a (µg L^{-1})	-0.42	0.24	0.16	0.07	-0.16	0.07	0.24	**-0.78**	0.07	-0.47	-0.07	-0.02	-0.02	-0.40	0.16	-0.36	0.02	-0.11	-0.28	-0.18	0.24	1.00								
Surf BG Cells (mL-1)	-0.02	0.11	0.29	-0.16	0.16	-0.16	0.29	-0.46	0.38	-0.16	-0.11	0.29	0.20	-0.09	-0.27	-0.50	-0.29	-0.33	-0.06	-0.22	0.20	0.51	1.00							
Surf DO (mg L-1)	**-0.51**	-0.20	-0.20	0.16	**-0.69**	0.33	-0.02	-0.14	0.16	-0.02	0.02	**-0.56**	-0.02	0.00	0.05	0.07	0.29	-0.11	**-0.83**	-0.13	-0.29	0.20	-0.11	1.00						
Bot Temp (°C)	**0.60**	0.33	0.16	-0.02	**0.73**	-0.38	-0.02	0.26	-0.16	0.02	-0.11	**0.51**	-0.07	0.13	-0.13	0.00	-0.20	0.24	**0.89**	0.11	0.17	-0.28	-0.06	**-0.94**	1.00					
Bot pH	-0.23	**-0.49**	-0.31	-0.27	-0.31	0.35	-0.20	0.10	0.09	-0.16	-0.24	**-0.49**	-0.20	**0.51**	0.13	0.06	0.02	-0.31	-0.28	**0.49**	-0.20	-0.24	-0.20	0.20	-0.16	1.00				
Bot Sp Cond (µS cm-1)	0.09	0.05	0.24	-0.24	0.38	0.02	0.05	-0.17	-0.01	-0.20	0.02	0.27	-0.16	-0.04	0.34	0.10	0.13	-0.05	0.28	0.27	**0.78**	0.11	0.07	**-0.51**	0.38	-0.05	1.00			
Bot Chl a (µg L-1)	-0.38	0.45	-0.02	0.09	-0.31	-0.16	0.09	**-0.60**	-0.05	-0.38	-0.16	0.02	0.16	**-0.51**	0.21	-0.40	-0.20	-0.09	-0.22	-0.27	0.07	**0.73**	0.33	0.20	-0.20	-0.16	-0.05	1.00		
Bot BG Cells (mL-1)	0.09	-0.16	-0.42	-0.02	-0.13	-0.06	-0.38	0.44	-0.01	0.31	-0.13	-0.16	-0.16	0.37	-0.43	0.13	0.20	0.02	-0.22	0.00	-0.24	-0.29	-0.16	0.42	-0.16	-0.05	-0.38	-0.27	1.00	
Bot DO (mg L-1)	-0.45	-0.13	-0.16	-0.13	**-0.60**	0.20	0.02	-0.02	0.02	0.13	0.13	-0.35	0.09	-0.04	0.26	0.17	0.16	-0.24	**-0.67**	-0.05	-0.38	-0.07	-0.20	**0.64**	**-0.73**	0.27	-0.35	0.05	0.16	1.00

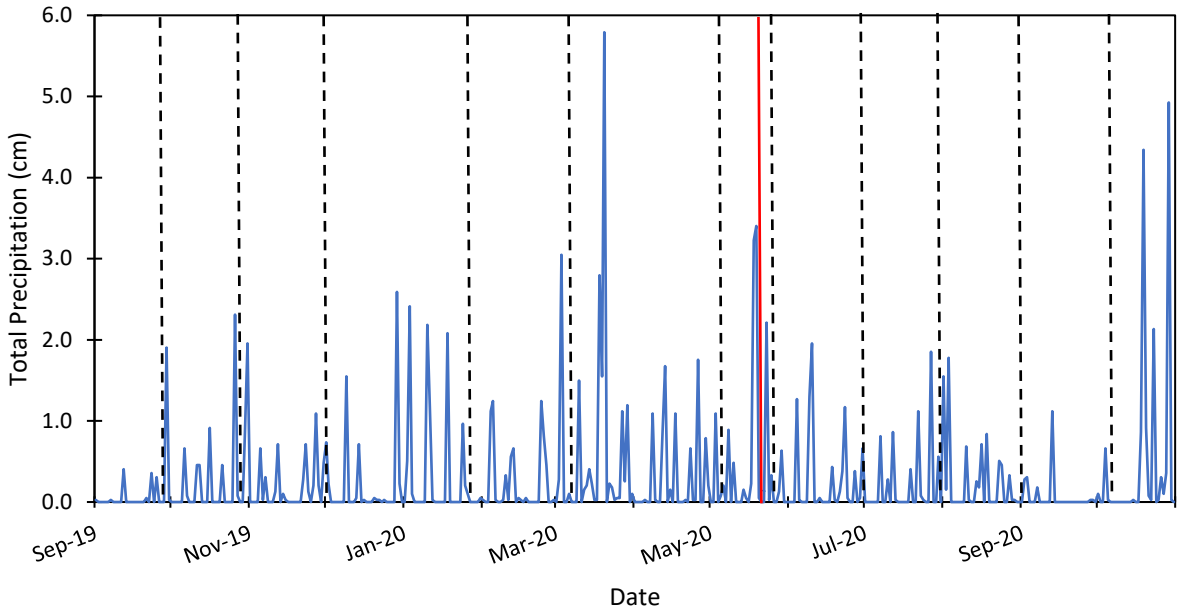

Figure 4. Total daily precipitation amounts between September 1, 2019, and October 31, 2020. Precipitation data was collected from the Xenia weather station on Weather Underground. Black dashed lines = sampling event, red solid line = fertilizer application.

Table 8. Ambient nutrient data collected at each sediment sampling event. Units are µM N (or P). Samples below detection limit are reported as less than that method's detection limit.

Sampling Date	SRP	NH_4^+	NO_2^-	NO_3^-	Urea
9/30/19	0.012	<0.200	<0.036	0.468	1.95
10/29/19	0.030	2.258	<0.036	0.045	0.80
12/2/19	0.023	5.340	0.049	0.828	1.26
1/27/20	0.050	0.828	0.135	1.947	0.592
3/9/20	0.024	<0.200	<0.036	0.195	0.742
5/6/20	0.042	0.024	<0.036	0.209	4.47
5/26/20	0.032	<0.200	0.044	0.156	2.55
7/1/20	0.037	3.806	0.156	0.669	3.04
7/28/20	0.047	<0.200	<0.036	0.203	0.956
9/1/20	0.042	<0.200	<0.036	0.086	0.336
10/6/20	0.051	<0.200	<0.036	0.337	0.702
Mean (±SE)	0.035 (±0.004)	1.114 (±0.968)	0.077 (±0.023)	0.468 (±0.158)	1.582 (±0.956)

urea concentrations ranged from 0.336 to 4.47 µM (median = 0.956 µM), peaking on May 6, 2020.

Sediment Nutrient Fluxes

Sediments were a source of NH_4^+ to the overlying water in C and N cores (Figure 5). NH_4^+ efflux was generally lower in the N cores compared to the C cores, although not statistically robust (Wilcoxon Signed-Rank, $p > 0.05$). NH_4^+ efflux from C cores increased during spring, peaking on May 26, 2020 (125 µmol N m^{-2} h^{-1}), then decreased during summer. NH_4^+ influx (-14.0 µmol N m^{-2} h^{-1}) was observed on September 30, 2019. NH_4^+ fluxes in N cores also increased during spring, peaking on May 26, 2020 (66.4 µmol N m^{-2} h^{-1}). NH_4^+ flux was lower in A cores compared to C cores (Wilcoxon Signed-Rank, $p < 0.05$) during all incubations. Net NH_4^+ influx in A cores peaked during fall and winter on October 6, 2020 (-98.9 µmol N m^{-2} h^{-1}), while net NH_4^+ efflux peaked during spring and summer (31.5 µmol N m^{-2} h^{-1}) on May 6, 2020.

Sediments were generally a source of dissolved SRP to the overlying water in C cores. However, sediments varied between a source and sink in the A and N cores (Figure 6). SRP flux was generally lower in A cores than C cores for all incubations that occurred between September 30, 2019 and May 6, 2020, although not statistically robust (Wilcoxon Signed-Rank, $p > 0.05$). Also, from the May 6 to October 6, 2020, incubations, SRP fluxes in N cores were lower than in C cores (Wilcoxon Signed-Rank, $p < 0.05$). Following the fertilizer application on May 26, 2020, SRP effluxes in both C and A cores peaked, with efflux in A cores higher than those in C cores (Wilcoxon Signed-Rank, $p < 0.05$), while a net influx was observed in N cores.

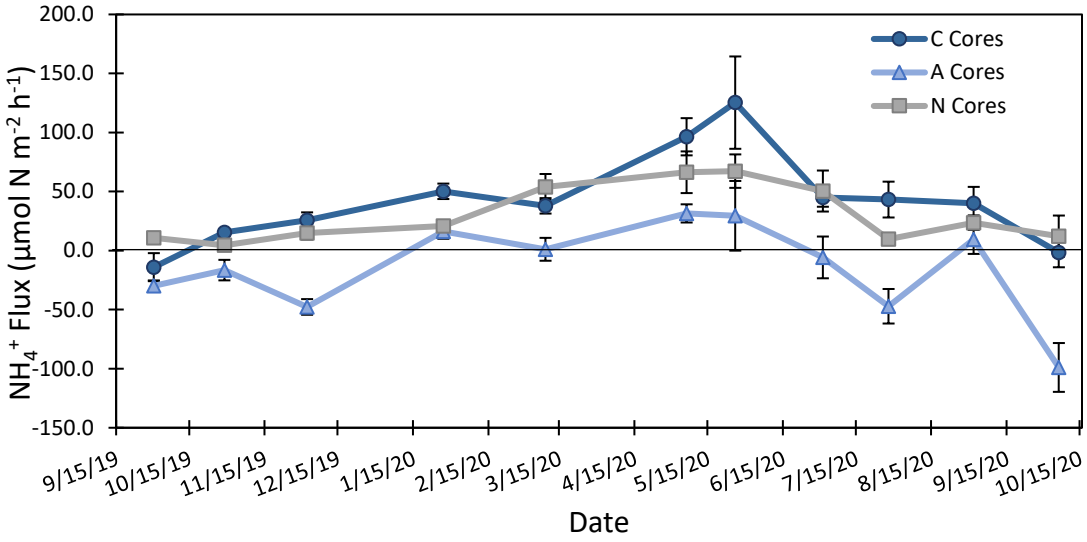

Figure 5. Mean (± SE) NH_4^+ fluxes from triplicate unamended control (C), $^{15}NH_4^+$ (A), and $^{15}NO_3^-$ (N) amended sediment cores. A positive value represents efflux from sediments, while a negative value represents influx into sediments.

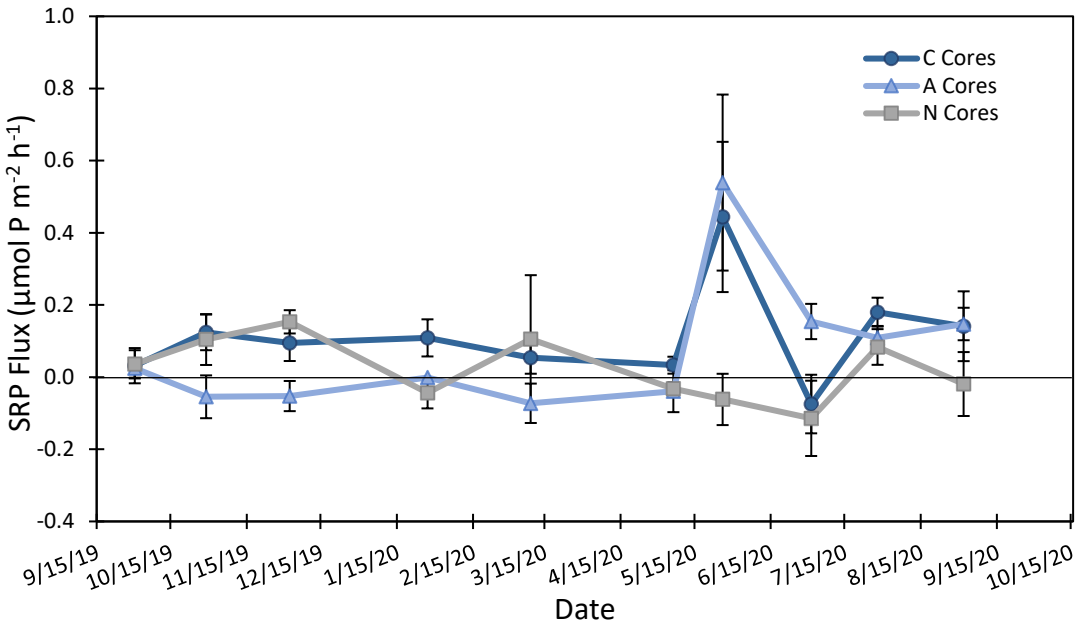

Figure 6. Mean (± SE) SRP fluxes from triplicate unamended control (C), $^{15}NH_4^+$ (A), and $^{15}NO_3^-$ (N) amended sediment cores. A positive value represents an efflux from the sediment while a negative value represents an influx into the sediment.

Sediments were generally a source of NO_3^- to the overlying water in C and A cores (Figure 7). Nitrate efflux peaked at 27.3 and 46.4 µmol N m^{-2} h^{-1} on May 26, 2020, in C and A cores, respectively. Nitrate effluxes in A cores were greater than in C cores throughout all incubations (Wilcoxon Signed-Rank, $p < 0.05$). N cores exhibited an influx of NO_3^- up to -237 µmol N m^{-2} h^{-1} on July 28, 2020, and an overall mean influx of -91.3 ± 18.4 µmol N m^{-2} h^{-1}. As expected, N core NO_3^- fluxes were consistently lower than those in C cores (Wilcoxon Signed-Rank, $p < 0.05$).

Sediments were a consistent source of NO_2^- to the overlying water in all treatments (Figure 8). All sediment NO_2^- effluxes exhibited a seasonal trend, with higher fluxes during spring and summer and lower fluxes during fall and winter. NO_2^- effluxes peaked on July 1, 2020, with fluxes of 28.6 (± 5.86), 32.3 (± 3.53), and 42.7 (± 14.3) µmol N m^{-2} h^{-1} in C, A, and N cores, respectively. Notably, NO_2^- fluxes in A and N cores were both higher than in C cores during this incubation. In addition to July 1, 2020, C cores also exhibited a higher efflux (28.6 ± 11.4 µmol N m^{-2} h^{-1}) on May 26, 2020 (fertilizer application four days prior to sampling), while NO_2^- fluxes in A and N cores remained lower. NO_2^- effluxes in A cores were higher than in C cores during most incubations (Wilcoxon Signed-Rank, $p < 0.05$). NO_2^- fluxes in N cores were generally higher than C cores, although the difference was not statistically robust (Wilcoxon Signed-Rank, $p > 0.05$). NO_2^- fluxes in N cores were positively correlated with net $^{29}N_2$ ($\tau = 0.6$, $p = 0.01$) and net $^{30}N_2$ gas fluxes ($\tau = 0.53$, $p = 0.024$) in N cores.

Sediments were a consistent source of urea to the overlying water in all incubations except for C cores on October 6, 2020 (Figure 9). Fluxes were generally indistinguishable between the C (mean: 4.73 ± 1.44 µmol N m^{-2} h^{-1}), A (5.15 ± 1.87 µmol N m^{-2} h^{-1}),

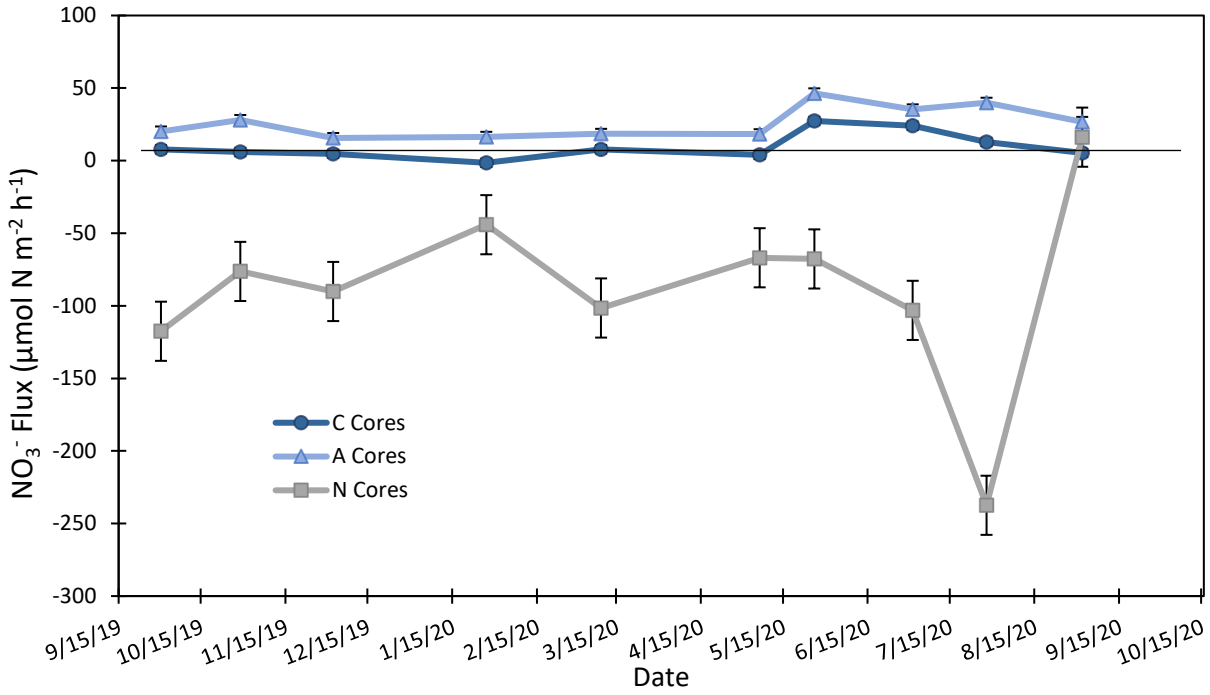

Figure 7. Mean (±SE) NO_3^- flux from triplicate control (C), $^{15}NH_4^+$ (A), and $^{15}NO_3^-$ (N) amended sediment cores. A positive value represents an efflux from the sediment, while a negative value represents an influx into the sediment.

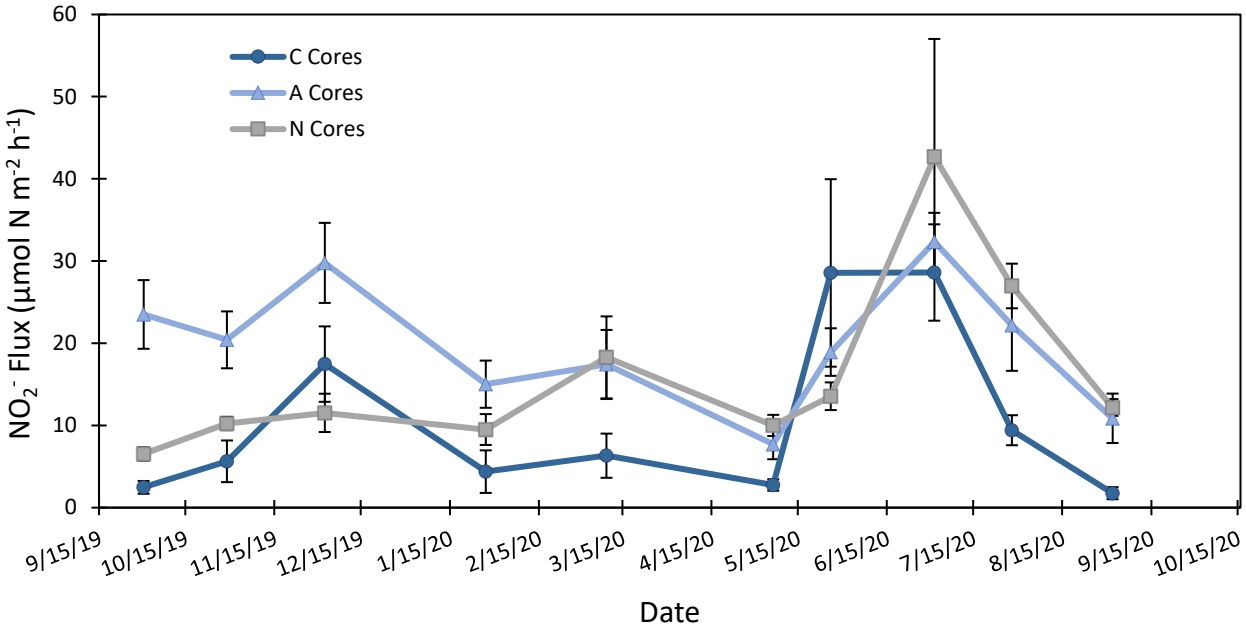

Figure 8. Mean (±SE) NO_2^- flux from triplicate control (C), $^{15}NH_4^+$ (A), and $^{15}NO_3^-$ (N) amended sediment cores. A positive value represents an efflux from the sediment, while a negative value represents an influx into the sediment.

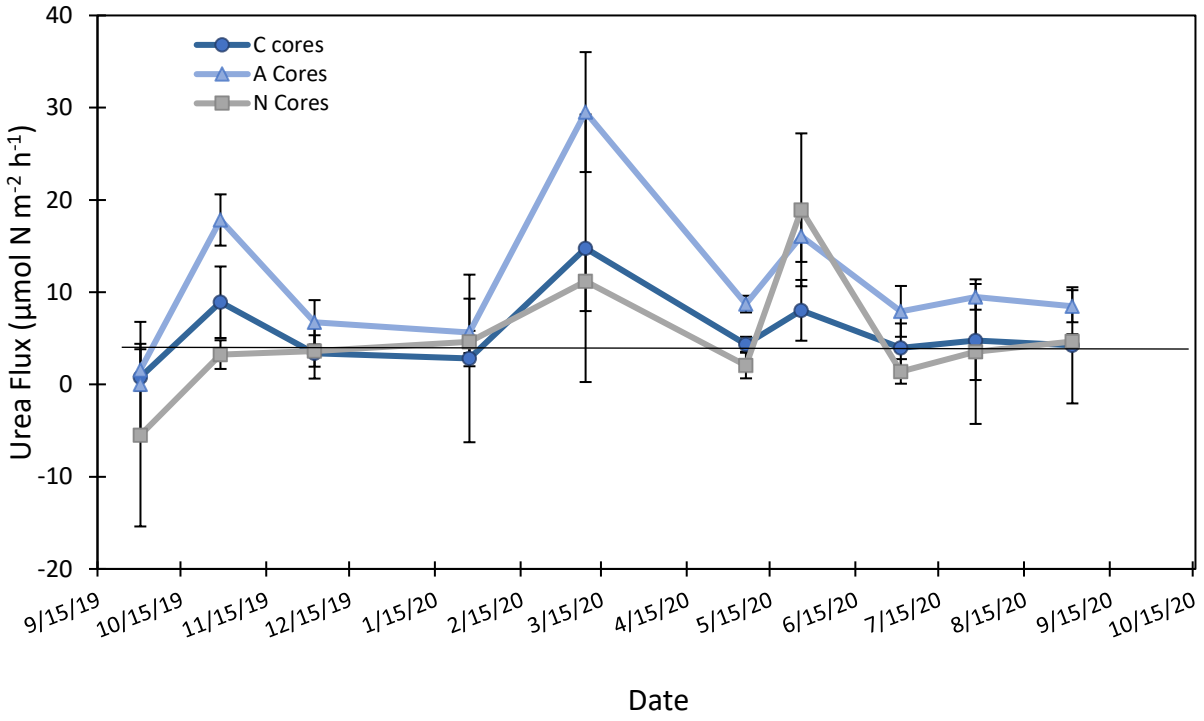

Figure 9. Mean (± SE) urea fluxes from triplicate control (C), $^{15}NH_4^+$ (A), and $^{15}NO_3^-$ (N) amended sediment cores. A positive value represents efflux from sediments, while a negative value represents influx into sediments.

and N (5.67 ± 1.18 µmol N m^{-2} h^{-1}) cores throughout all incubations. Urea fluxes peaked in C and N cores to 14.8 (± 6.50) and 14.5 (± 3.63) µmol N m^{-2} h^{-1}, respectively, on March 9, 2020. Urea fluxes in A cores peaked during the May 26, 2020 (18.9 ± 8.29 µmol N m^{-2} h^{-1}) incubation, which followed a fertilizer application. Urea efflux in A cores during this incubation was higher than in C cores, while urea efflux in N cores remained lower. Sediments acted as a urea sink on October 6, 2020, in C cores, and urea fluxes ranged from -4.0 (± 2.25) to 14.8 (± 6.5; median = 4.24) µmol N m^{-2} h^{-1} in C cores.

Unamended (C) cores are assumed to represent *in situ* sediment function. Pond sediments were a consistent source of bioavailable N and P to the overlying water during all sampling events (Figure 10). Ammonium and urea fluxes were negative (indicating sediment influx) on October 6, 2020, and NH_4^+ flux was also negative on September 30, 2019. Total bioavailable N efflux (DIN + urea) ranged from 36.0 to 189 µmol N m^{-2} h^{-1}. The highest efflux was observed on May 26, 2020. NH_4^+ generally made up the largest proportion of total N efflux in C cores during each incubation.

A and N cores are assumed to represent sediment function when a pulse of N is applied. Net uptake of NO_3^- in N cores was observed, with influxes ranging between -67.0 (± 15.8) and -237 (± 12.2) µmol N m^{-2} h^{-1} (Figure 11). Pond sediments were a consistent source of NH_4^+, NO_2^-, and urea during all incubations. However, following $^{15}NO_3^-$ addition, pond sediments functioned as a net N sink during seven of the eleven incubations, ranging between -4.8 and -196 µmol N m^{-2} h^{-1} on January 1 and July 28, 2020, respectively.

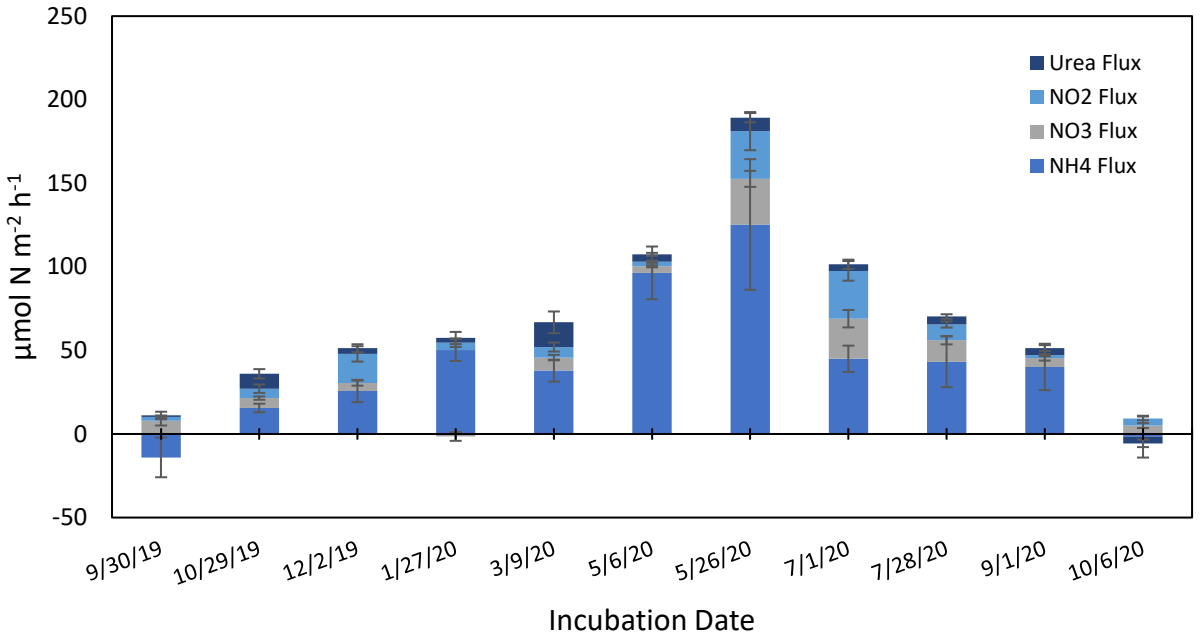

Figure 10. Mean urea, nitrite (NO_2^-), nitrate (NO_3^-), and ammonium (NH_4^+) fluxes from triplicate unamended control (C) sediment cores. A positive value represents efflux from sediments, while a negative value represents influx into sediments.

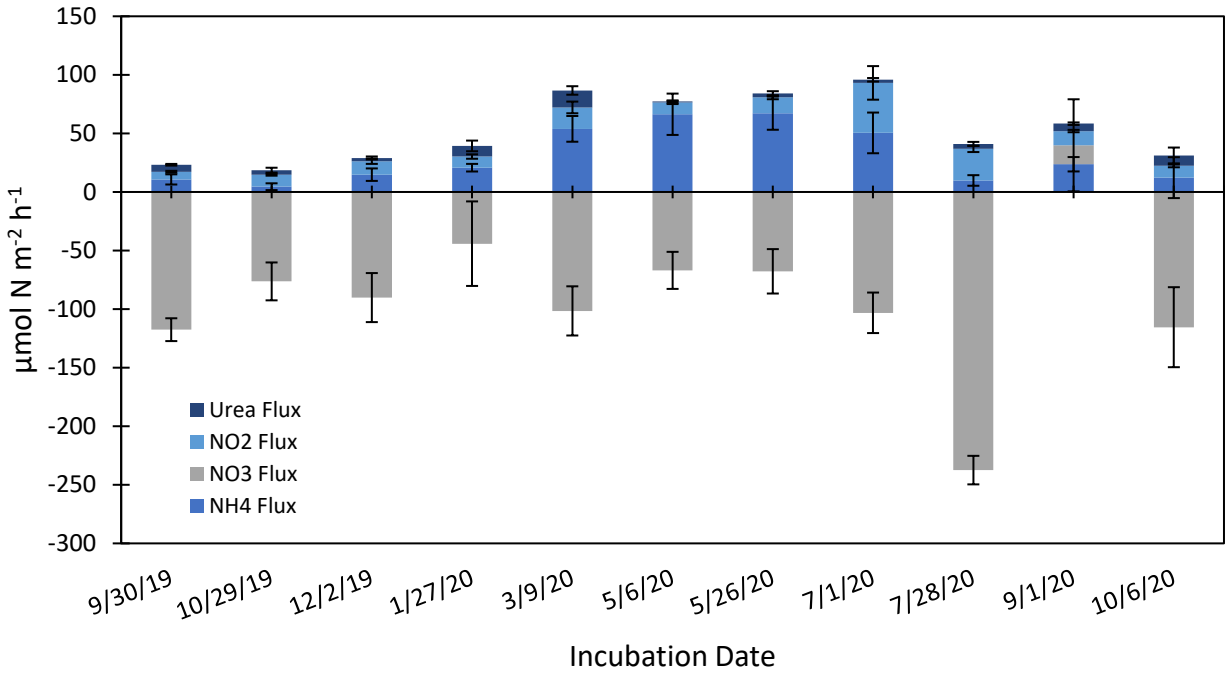

Figure 11. Mean urea, nitrite (NO_2^-), nitrate (NO_3^-), and ammonium (NH_4^+) fluxes from triplicate $^{15}NO_3^-$ (N) amended sediment cores. A positive value represents efflux from sediments, while a negative value represents influx into sediments.

Sediment Dissolved Gas Fluxes

Sediment Oxygen Demand

SOD varied seasonally in the three treatments (C, A, and N), ranging from 683 to 2,421 µmol O_2 m^{-2} h^{-1} (Figure 12). SOD for all cores increased during the warmer months. SOD in C cores was positively correlated with surface ($\tau = 0.61$, $p = 0.022$; Table 7) and bottom ($\tau = 0.6$, $p = 0.016$; Table 7) water temperature. SOD in C and A cores peaked earliest in the year on May 26, 2020, although SOD in N cores remained lower. SOD in N cores peaked later in the summer on July 28, 2020, and was higher than in C cores, while SOD in A cores remained lower. Between December 2, 2019, and March 9, 2020, SOD in N cores was higher than in C cores. SOD in all cores were higher in September and October 2020 than in September and October 2019.

Possible Anammox

On average, anammox may have contributed 2.56% (± 0.19%) of total N_2 production (Figure 13). Anammox contribution peaked at 8.06% on May 26, 2020. The lowest contribution was observed on May 6, 2020, with 0.77% of total N_2 production. NO_2^- and NH_4^+ fluxes in A cores were negatively correlated ($\tau = -0.6$, $p = 0.01$). Absolute rates of $^{29}N_2$ production in A cores were low (0.21 ± 0.08 to 8.34 ± 1.71 µmol N m^{-2} h^{-1}; Figure 14) compared to potential denitrification rates (39.6 ± 12.2 to 171 ± 24.5 µmol N m^{-2} h^{-1}).

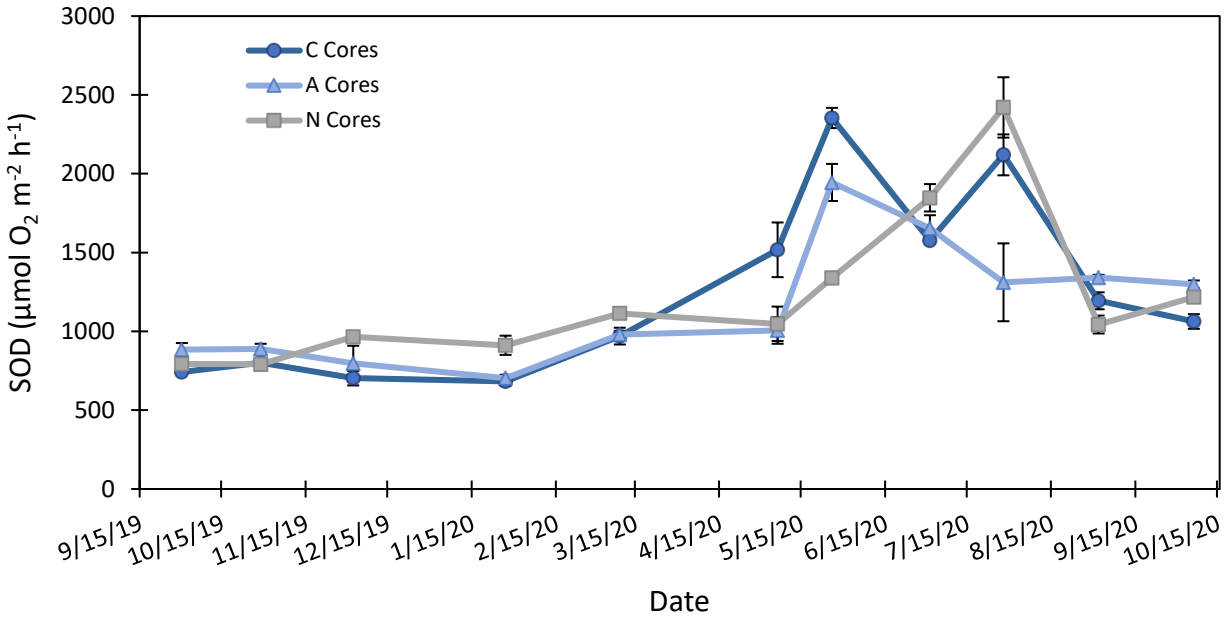

Figure 12. Mean (± SE) sediment oxygen demand (SOD) in unamended control (C), $^{15}NH_4^+$ (A), and $^{15}NO_3^-$ (N) triplicate sediment cores from sediment core incubations from September 30, 2019, to October 6, 2020.

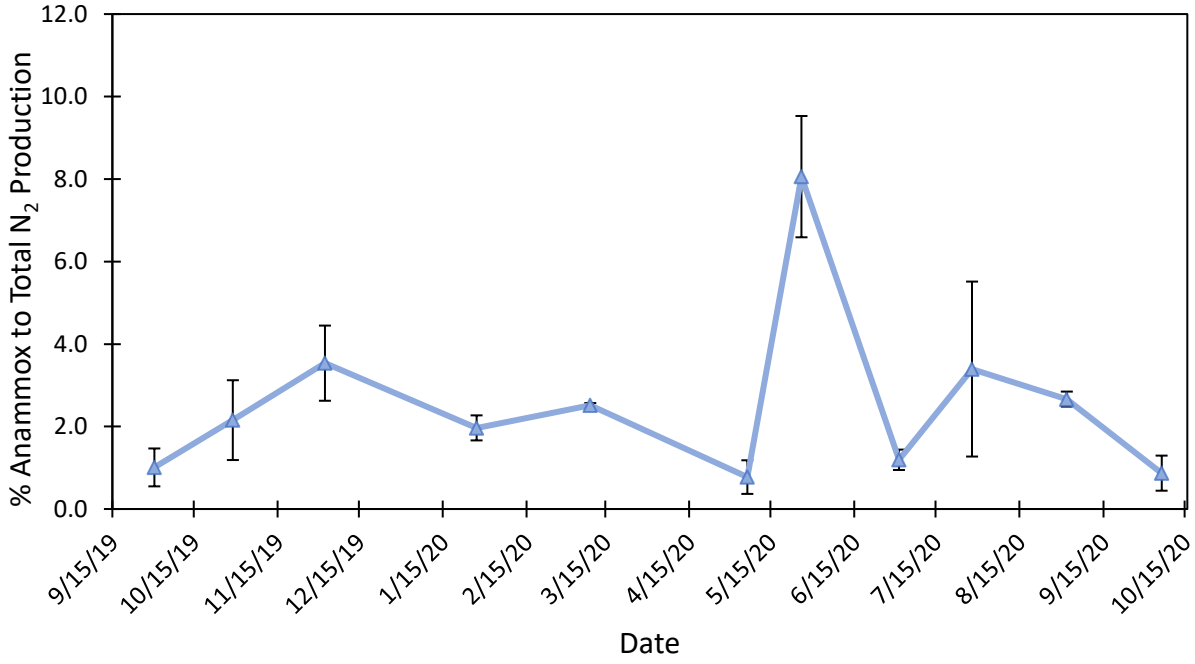

Figure 13. Mean (± SE) percent contribution of possible anammox to total N_2 production during monthly incubations from September 30, 2019, to October 6, 2020. The percentages were calculated by determining the ratio of $^{29}N_2$ gas produced in $^{15}NH_4^+$-amended cores to the $^{28+29+30}N_2$ gas produced, plus any calculated N fixation, in $^{15}NO_3^-$-amended cores.

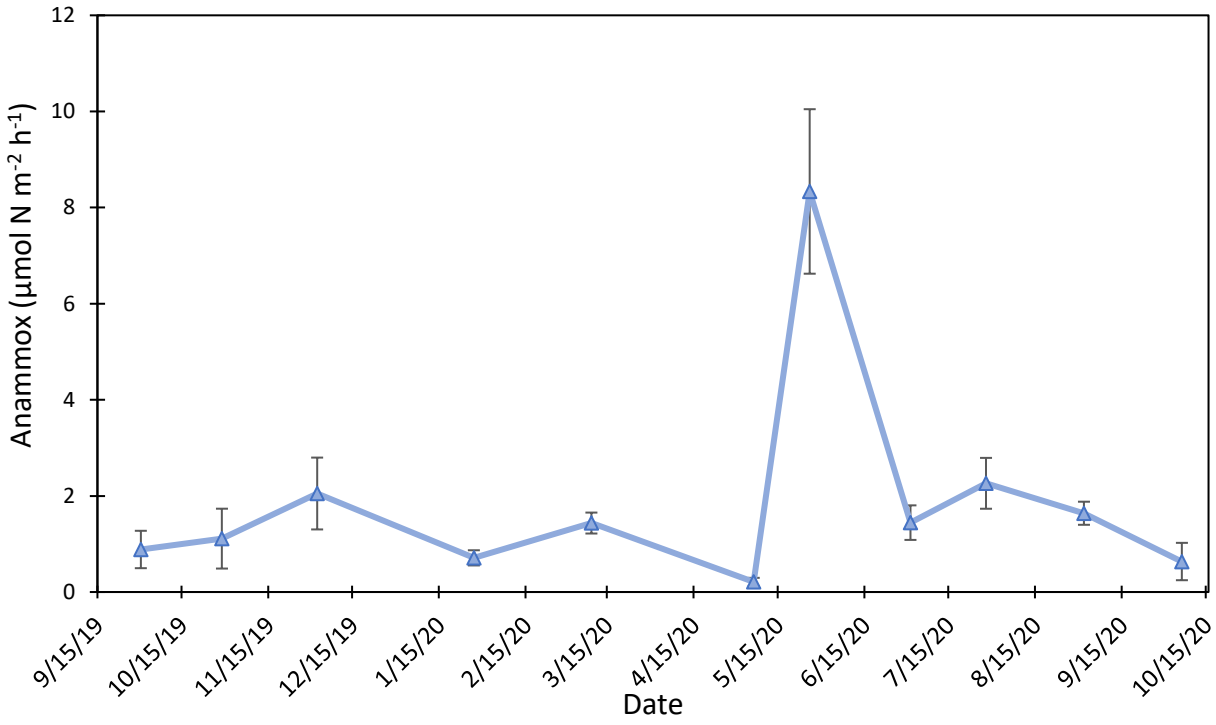

Figure 14. Mean (± SE) $^{29}N_2$ production (possible anaerobic ammonium oxidation (anammox) rates in $^{15}NH_4^+$ (A) amended triplicate sediment cores.

$^{28}N_2$ Flux (C cores) and Potential Denitrification (N cores)

Net N fixation was observed in most of the unamended C cores, except on September 30, 2019, and May 26, 2020 (Figure 15). Net denitrification in C cores on September 30, 2019, followed a rainfall event totaling 1.91 cm the day prior to sampling. The May 26, 2020 sampling followed a fertilizer application that occurred four days prior, with 2.57 cm of rain falling between those events. Net N fixation rates in C cores ranged from -2.56 µmol N m^{-2} h^{-1} on October 29, 2019 to -117 µmol N m^{-2} h^{-1} on May 6, 2020. Potential denitrification rates in N cores ranged from 39.6 µmol N m^{-2} h^{-1} on January 27, 2020, to 171 µmol N m^{-2} h^{-1} on July 28, 2020. Potential denitrification rates increased during warmer months and were positively correlated with surface ($\tau = 0.89$, $p < 0.001$; Table 7) and bottom ($\tau = 0.73$, $p = 0.003$; Table 7) water temperature. Potential denitrification rates were also positively correlated with SOD in N cores ($\tau = 0.67$, $p = 0.004$) and NO_3^- flux in C cores ($\tau = 0.6$, $p = 0.01$; Table 7), while NO_3^- flux in N cores was negatively correlated to potential denitrification rates ($\tau = -0.49$, $p = 0.036$).

Best Estimate of In Situ Denitrification

The best estimate of *in situ* denitrification was calculated by summing net $^{28}N_2$ fluxes from C cores and calculated N fixation from N cores. *In situ* denitrification was positive during all incubations and remained below 100 µmol N m^{-2} h^{-1}, except for a peak on May 26, 2020 (184 µmol N m^{-2} h^{-1}; Figure 16).

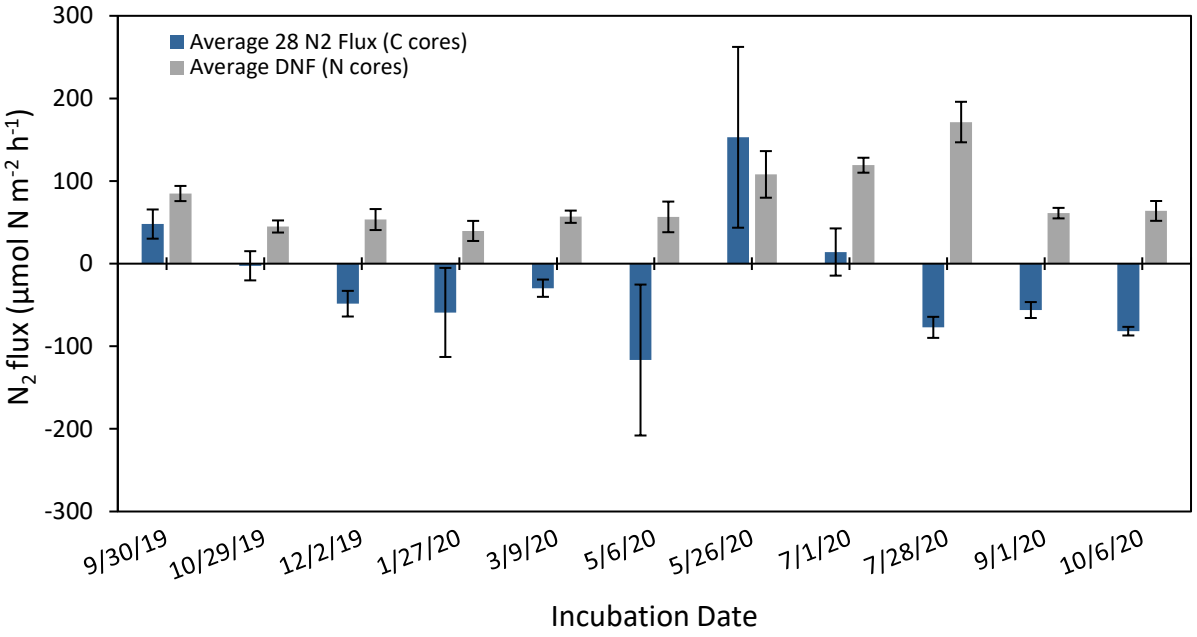

Figure 15. Mean (± SE) $^{28}N_2$ flux (C cores) and potential denitrification (N cores). A positive $^{28}N_2$ flux in C cores represents net denitrification, while a negative flux represents net N fixation. Potential denitrification was calculated by adding $^{28}N_2$, $^{29}N_2$, and $^{30}N_2$ gases produced to any N fixation calculated from N cores.

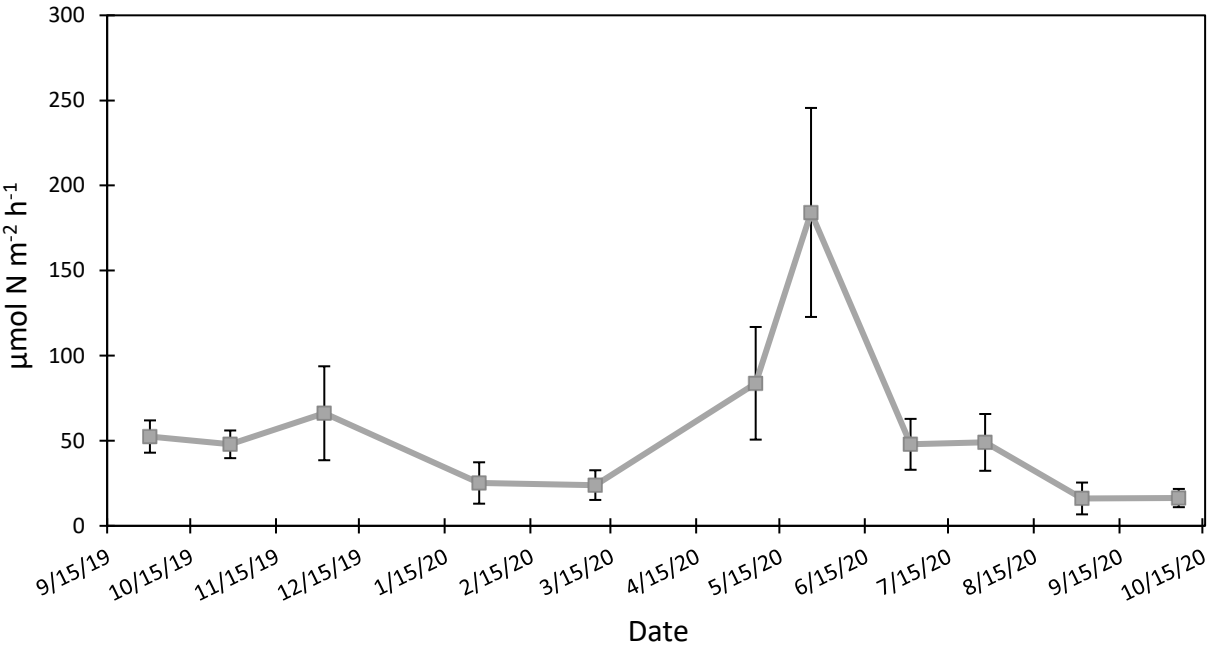

Figure 16. Mean (± SE) *in situ* denitrification rates were calculated from net $^{28}N_2$ flux in triplicate unamended control (C) cores plus any N fixation calculated from triplicate $^{15}NO_3^-$-amended cores.

Dissimilatory Nitrate Reduction to Ammonium (DNRA)

Potential DNRA was detectable but low in seven of eleven incubations (Figure 17) and rates ranged from 0.34 to 4.19 µmol N m^{-2} h^{-1} (mean = 1.32 ± 0.4 µmol N m^{-2} h^{-1}). Higher rates were observed in spring and early summer, with potential DNRA rates peaking on April 6, 2020. DNRA was positively correlated with NH_4^+ flux in C cores ($\tau = 0.60$, $p = 0.013$; Table 7) and N cores ($\tau = 0.48$, $p = 0.046$). DNRA contributed 0 to 20.6 (± 20.4)% (median = 1.1%) to total NH_4^+ production (Figure 18).

Nitrogen Fixation (N Cores)

N fixation occurring simultaneously with denitrification was observed throughout the year (except September 30, 2019), with an overall average of 68.7 ± 10.2 µmol N m^{-2} h^{-1} (Figure 19). N fixation rates ranged from undetectable on September 30, 2019, to 118 µmol N m^{-2} h^{-1} on December 2, 2019 (median = 64.7 µmol N m^{-2} h^{-1}). N fixation was negatively correlated with net $^{28}N_2$ fluxes in C cores ($\tau = -0.64$, $p = 0.006$; Table 7) and N cores ($\tau = -0.85$, $p < 0.001$). N fixation was also negatively correlated with surface water temperature ($\tau = -0.56$, $p = 0.037$; Table 7).

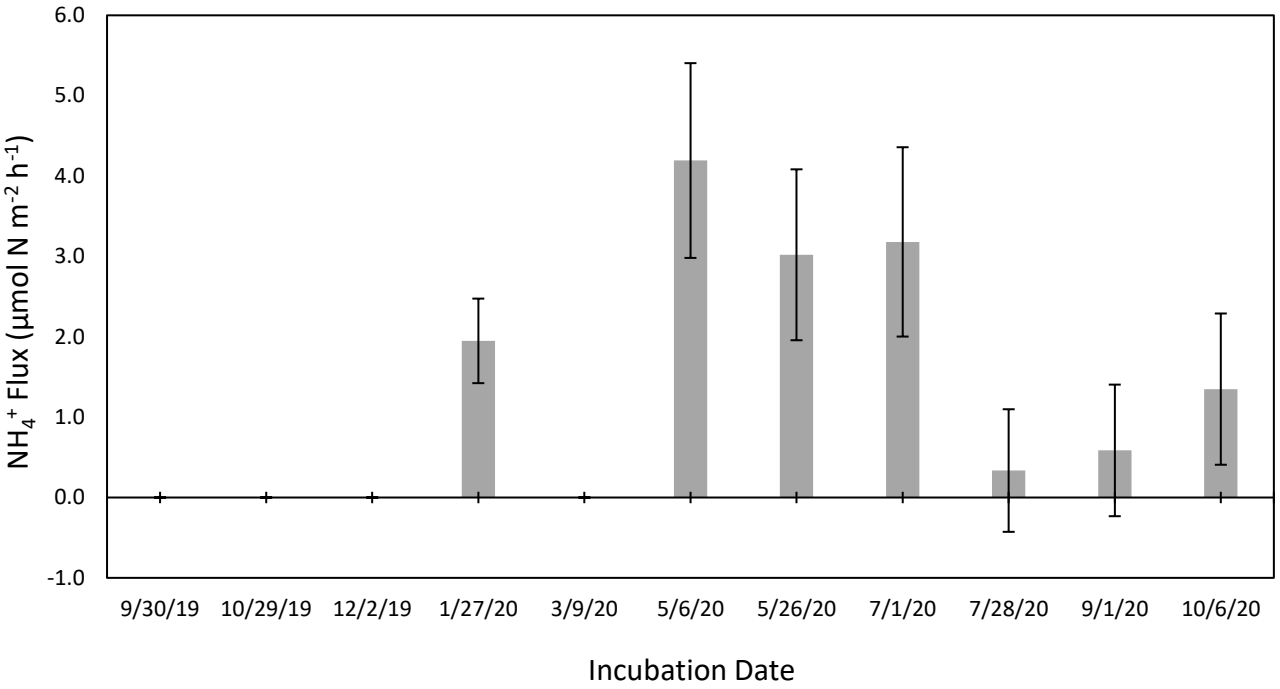

Figure 17. Mean (± SE) potential dissimilatory NO_3^- reduction to NH_4^+ (DNRA) rates measured as $^{15}NH_4^+$ production from triplicate $^{15}NO_3^-$-amended cores.

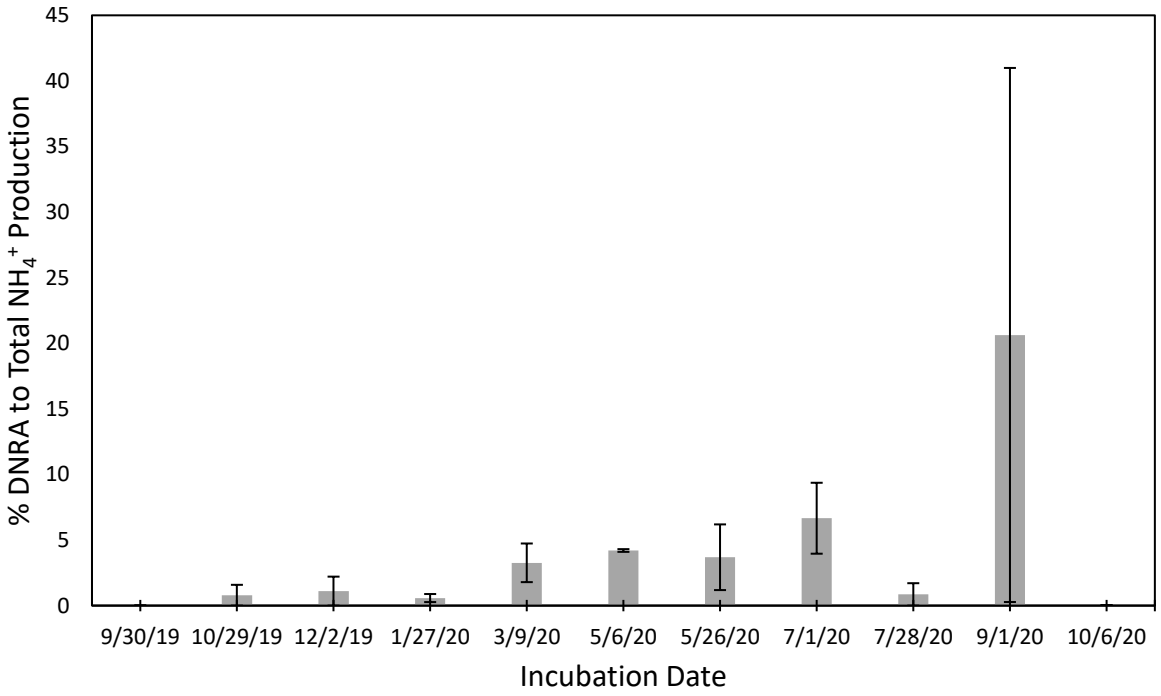

Figure 18. Mean (± SE) percent potential dissimilatory NO_3^- reduction to NH_4^+ (DNRA) contribution to total NH_4^+ production from triplicate $^{15}NO_3^-$-amended cores.

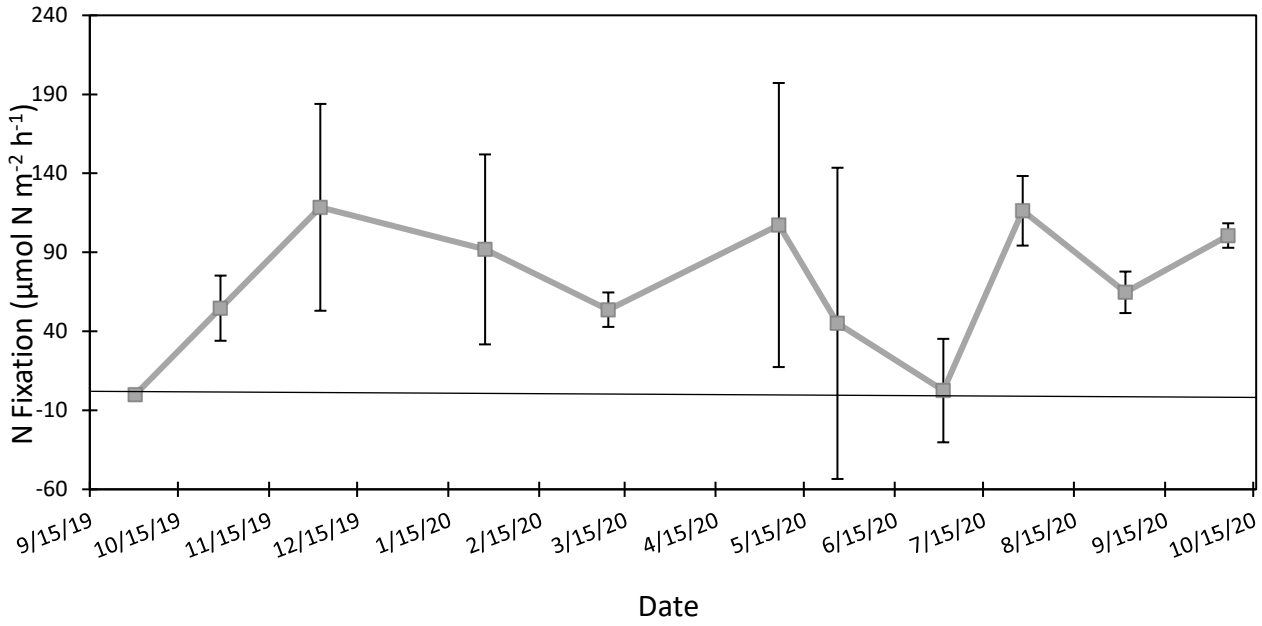

Figure 19. Mean (± SE) Nitrogen (N) fixation rates calculated from triplicate $^{15}NO_3^-$-amended sediment cores.

IV. DISCUSSION

This study showed that settling pond sediments supported active microbial processes, including denitrification, anammox, and nitrification, that were often consistent with substrate limitation. Settling pond sediments usually exhibited net N fixation, but net denitrification occurred in some cases after rain events or fertilizer application. During our sampling events, pond sediments functioned as a net source of N, but the sediments were important in removing N pulses from fertilizer runoff and precipitation. Wetland and settling pond monitoring data showed that, under high N loading, the wetland was not effective at removing N (likely due to a shorter residence time), while the settling pond rapidly removed N loads. Net denitrification was observed in pond sediments following a N fertilizer application in May 2020, and potential denitrification rates showed that sediments were capable of denitrifying excess NO_3^- when added. Given more frequent and higher N loading, N lost through denitrification could offset N fixation, suggesting that settling ponds are a valuable asset to agriculture nutrient mitigation systems.

Seasonal Trends

Microbial activity followed expected seasonal trends, with higher rates in summer, and lower rates in winter. SOD is indicative of aerobic respiration of organic matter in sediments (Seiki et al., 1994), and higher SOD was observed in spring and summer (Figure 12). High summer SOD suggested sufficient organic matter for aerobic

respiration (including plant detritus and fish waste), despite the young age of the pond (built in 2016). The pond water column remained oxygenated during summer, despite high SOD. Peak NH_4^+ efflux in unamended C cores coincided with peak SOD at the end of May 2020 (Figures 5, 12). Nitrogen fertilizer was applied on the adjacent field four days prior to the May 2020 sampling (Table 1), which likely stimulated microbial activity. Precipitation of 2.57 cm fell on the area between fertilizer application and sampling, which likely supplied the pond with N (Figure 4). Lower SOD was observed in fall and winter, coincident with lower temperatures and suggests that organic matter may have limited SOD later in the season (McCarthy et al., 2016). Fall and winter SOD remained consistent, suggesting that microbes maintained their ability to respire at colder temperatures. SOD in the settling pond (683 – 2,350 μmol O_2 m^{-2} h^{-1}) was within the range (312 – 3,400 μmol O_2 m^{-2} h^{-1}) of those reported in other studies of freshwater wetlands and lakes (Boedecker et al., 2020; McCarthy et al., 2007, 2016; Scott et al., 2008).

Similar to SOD, potential denitrification rates (N cores) followed a seasonal trend (Figure 15), with higher rates during the warmer months. Temperature is a well-documented driver of denitrification rates (Seitzinger, 1988) and has been reported in numerous other studies across a wide range of ecosystems. Higher summer denitrification rates were observed in agriculture drainage ditches, in part due to enhanced denitrifier activity as a result of warmer water temperatures (She et al., 2018). Higher denitrification rates at warmer temperatures were also reported in a constructed wetland draining a row-crop landscape (Poe et al., 2003), and in agricultural pond sediment where a dramatic

increase was observed between 18–30°C, compared to 6–18°C (Li et al., 2010). These results underscore the importance of temperature as a driver of denitrification rates.

Net N_2 Gas Fluxes

Settling pond sediments were generally a source of N, with net N fixation observed in all C cores except for September 30, 2019, and May 26, 2020 (Figure 15). The balance between N fixation and denitrification is influenced by numerous factors, including O_2 concentration, supply of organic carbon, and NO_3^- availability (Seitzinger, 1988). Bottom water DO concentrations were negatively correlated with denitrification potential ($\tau = -0.60$, $p = 0.01$; Tables 6, 7; Figure 15), indicating that lower O_2 concentrations were conducive for denitrification to occur, as reported in numerous other studies of estuaries and freshwater lakes (Bruesewitz et al., 2011; Gardner et al., 2006). Organic matter was likely not the main limiting factor, as potential denitrification rates were positively correlated to SOD in N cores ($\tau = 0.67$, $p = 0.004$; Figures 12, 15). In addition, NH_4^+ flux was marginally correlated with SOD in C cores ($\tau = 0.42$, $p = 0.07$; Table 7; Figures 5, 12). SOD and NH_4^+ flux are both proxies for labile organic matter and microbial activity in sediments, suggesting that sufficient organic matter was available in the sediments for denitrifiers. Organic matter in the settling pond may be accumulating with age in the settling pond (Craft, 1996; Hernandez & Mitsch, 2007; Poe et al., 2003), as the baseline SOD increased over the course of the year between the sampling events in September and October of 2019 and 2020. (Figure 12).

Nitrate is likely the key limiting factor in the sediments of the settling pond, as potential denitrification rates (N cores) were positively correlated with NO_3^- fluxes in C cores ($\tau = 0.6$, $p = 0.01$; Table 7; Figures 7, 15). This relationship suggests that, under

normal conditions, NO_3^- was limiting denitrification, indicated by the positive NO_3^- flux in C cores. When given excess $^{15}NO_3^-$ (N cores), denitrifiers were stimulated and capable of removing the $^{15}NO_3^-$ pulse. In addition, NO_3^- fluxes in N cores were negatively correlated with potential denitrification rates (N cores; $\tau = -0.49$, $p = 0.036$), suggesting higher NO_3^- uptake at higher potential denitrification rates, indicative of direct denitrification (as opposed to coupled nitrification-denitrification). Nitrate availability is widely reported as a major driver of denitrification rates, including in agricultural drainage ditches. She et al. (2018) reported that denitrification rates were positively correlated to overlying water NO_3^- concentrations in these systems, and rates peaked in summer, coinciding with heavy runoff and high applications of N fertilizer. Furthermore, denitrification was enhanced in these sediments following NO_3^- additions in laboratory incubations, similar to results from $^{15}NO_3^-$ additions in this study. In another study of a stormwater wet pond (constructed to manage stormwater runoff in developed areas), low ambient NO_3^- concentrations corresponded to net N fixation, while pulses of high NO_3^- corresponded to net denitrification (Gold et al., in revision), and a similar pattern was reported in shallow, eutrophic flood-control impoundments (Grantz et al., 2012). Nitrate concentrations, then, can be the critical factor controlling whether net denitrification or net N fixation is observed.

It was hypothesized that pond sediments would exhibit net denitrification, as the settling pond is in an actively fertilized, agricultural landscape, but denitrification in the pond was NO_3^- limited most of the year. This conclusion was supported by the difference between net $^{28}N_2$ fluxes (C cores) and measurable potential denitrification rates (N cores) during all incubations following $^{15}NO_3^-$ addition (Figure 15). However, net denitrification

was observed twice in C cores, once after a 1.91 cm rain event (September 30, 2019), when N may have run off from the crop field into the pond, stimulating denitrification. Ambient NO_3^- concentration was low at this time (0.468 µM), likely because NO_3^- entering the pond was already denitrified and no longer present in the water column. Net denitrification was also observed following fertilizer application (6% ammonium, 6% potassium, and 24% phosphate; Table 1) in late May 2020. Fertilizer application occurred four days prior to sampling, and 2.57 cm of rain fell on the area between fertilizer application and sampling, which may have supplied the settling pond with N to stimulate denitrification (Figure 4). These results suggest that the settling pond has a microbial population capable of denitrifying higher NO_3^- loads, and that denitrification was dependent on NO_3^- load. In the absence of sufficient NO_3^-, pond sediments instead exhibited net N fixation (Fleischer et al., 1994; Poe et al., 2003; Seitzinger, 1988). These results align with other studies in reservoirs (Grantz et al., 2012; Richardson & Herrman, 2020), a freshwater wetland (Scott et al., 2008), and a stormwater wet pond (Gold et al., in revision), which also observed net N fixation and low rates of denitrification with low ambient NO_3^- concentrations.

The wetland and settling pond monitoring data further support that the settling pond was effective at removing high N loads. The entire system exhibited low NO_3^- concentrations in spring through fall, with little NO_3^- entering the system. However, higher ambient NO_3^- concentrations were observed in the wetland during winter and following fertilizer application in June 2019 (Table 2). At all sampling events during winter, the wetland was even a source of NO_3^- to the pond, indicated by higher NO_3^- concentrations in the wetland outlet versus inlet, which may be due to higher rates of

nitrification compared to denitrification, and less vegetative uptake of N (Huang et al., 2013). However, NO_3^- did not accumulate in the settling pond, indicating that the pond was effectively removing N and was more effective at N removal than the wetland.

The Fate of Nitrate

Results from this study supported the hypothesis that denitrification would be the primary N_2 removal process in the settling pond. These findings align with a study of another constructed agricultural pond, which found denitrification to be the dominant N_2 removal process over anammox (Uusheimo et al., 2018b). Anammox may have contributed, on average, 2.56% (± 0.19%) of total N_2 removal throughout the entire study, peaking at 8.06% on May 26, 2020 (coincident with overall higher rates of microbial activity post-fertilization and precipitation; Figure 13). The elevated possible anammox rates coincided with peak net NO_2^- efflux (28.6 μmol N m^{-2} h^{-1}), suggesting that incomplete N transformations provided additional substrate for the reaction (Figure 8). However, net NO_2^- and NH_4^+ effluxes suggested that their production exceeded uptake into the sediments, further supporting that N_2 production by anammox was minimal (Figures 5, 8). Overall, anammox may have been a minor component of total N removal in the settling pond, if it occurred, in alignment with other studies in freshwater reservoirs (Shen et al., 2017), lakes (Boedecker et al., 2020; McCarthy et al., 2016), and rivers (Zhao et al., 2013).

DNRA rates were detectable in seven of eleven incubations (Figure 17). In these incubations, DNRA contributed up to 7% of total NH_4^+ production and up to 6.7% to dissimilatory NO_3^- reduction (*[(DNRA / potential denitrification + DNRA) x 100]*). Higher DNRA rates were observed in the Fondriest settling pond when NO_3^-

concentrations were low ($\tau = 0.13$, $p = 0.576$; Table 7) and SOD (a proxy for organic matter) was high ($\tau = 0.37$, $p = 0.129$; Table 7), although DNRA rates were not robustly correlated to either parameter. Higher NH_4^+ fluxes were observed during these incubations (May 6, May 26, and July 1, 2020), and NH_4^+ fluxes were positively correlated to DNRA in N cores ($\tau = 0.48$, $p = 0.046$), suggesting that DNRA may be contributing to higher NH_4^+ effluxes. The July 1, 2020 incubation had measurable DNRA of 3.2 μmol N m^{-2} h^{-1} and coincided with one of the highest ambient NH_4^+ concentrations observed in the settling pond (3.8 μmol L^{-1}). However, the potential DNRA rate was likely too low to account for this NH_4^+ concentration, since total NH_4^+ flux in C cores on this date was much higher (45.2 ± 7.86 μmol N m^{-2} h^{-1}). The higher NH_4^+ concentration observed on this date may have instead resulted from runoff from a rain event (0.66 cm) the day prior (Figure 4), or remineralization of organic matter settled to the sediment surface. These results suggest that, although DNRA rates were measurable at times, it was a minor contributor to NO_3^- removal in the settling pond.

DNRA contributed up to 56% of dissimilatory NO_3^- reduction in various coastal and freshwater systems (Gardner et al., 2006; Jiang et al., 2020; McCarthy et al., 2016; Rahman et al., 2019; Scott et al., 2008; Washbourne et al., 2011), but DNRA is generally considered a minor dissimilatory NO_3^- removal process compared to denitrification in freshwater systems. In these studies, DNRA was more important than denitrification under high carbon, low NO_3^- conditions (Jiang et al., 2020; McCarthy et al., 2016; Rahman et al., 2019; Washbourne et al., 2011) and under highly reducing conditions, where sulfide was present and could inhibit nitrification and denitrification (Gardner et al., 2006; Scott et al., 2008).

Several different factors control the balance between DNRA and denitrification. Sediment organic carbon was the primary factor influencing DNRA rates in Chinese eutrophic lakes (Jiang et al., 2020), while temperature and NO_3^- concentrations determined the relative importance of DNRA versus denitrification in constructed stormwater urban wetlands (Rahman et al., 2019). DNRA became more important at low temperatures and low NO_3^- in these wetland systems. Free sulfides can also be an important control, as observed in an oligotrophic stream-lake system (Washbourne et al., 2011). The presence of free sulfides suggested that denitrification may have been suppressed, while DNRA was enhanced. In addition, the presence of macrophytes can favor DNRA due to enhanced carbon availability and O_2 levels. DNRA maintains bioavailable N in the system, where it can fuel primary production, whereas denitrification results in permanent removal of bioavailable N from the system; thus, the range of controls influencing the balance between DNRA and denitrification highlights the importance of continued investigation to better understand conditions that favor each pathway.

Sediment Nutrient Fluxes

Pond sediments were a source of all measured nutrients (NH_4^+, NO_3^-, NO_2^-, SRP, urea) to the overlying water column throughout the year. Results from N cores can be used to help understand how pond sediments respond to pulses of N from the watershed. Pond sediments were a sink for added $^{15}NO_3^-$ in all but one incubation and released NO_2^-, NH_4^+, and urea (Figure 11). Nitrite, NH_4^+, and urea effluxes in N cores were not different from those in C cores, suggesting that nutrient releases were neither stimulated nor reduced by $^{15}NO_3^-$ addition. Overall, sediments in N cores were a net sink for N (DIN +

urea flux), with high NO_3^- uptake offsetting the N released in all but three incubations during the study (May 6, May 26, and September 1, 2020). These observations align with reservoir and pond studies from agricultural landscapes, which have reported that these systems effectively remove N (David et al., 2006; Powers et al., 2015; Tournebize et al., 2015). Furthermore, potential denitrification rates (range: 45 to 171 µmol N m^{-2} h^{-1}; Figure 15) in pond sediments were similar in magnitude to NO_3^- influxes in N cores (range: -44 to -237 µmol N m^{-2} h^{-1}; Figure 7), suggesting that the majority of NO_3^- was denitrified and removed as N_2 gas. In the three incubations where an overall N efflux was observed (N cores), NH_4^+ fluxes comprised 40 – 46% of total DIN + urea flux, while the proportion of NH_4^+ flux remained below 28% in other incubations, suggesting that remineralization activity exceeded nitrification during these incubations. NO_3^- efflux in N cores was observed only on September 1, 2020, indicating that nitrification exceeded direct denitrification (Seitzinger 2008).

Ammonium and urea were released by sediments in unamended C cores, as hypothesized, likely associated with remineralization of organic matter (Figures 5, 9; Berman et al., 1999). However, NO_3^- was also released from sediments into the overlying water column during all incubations (Figure 7). Nitrate effluxes in C cores are likely explained by nitrification rates exceeding denitrification and DNRA, or uncoupled nitrification-denitrification resulting in net release of NO_3^- (Boedecker et al., 2020). The water column in the settling pond remained oxygenated (4.9 to 14.0 mg L^{-1}), providing favorable conditions for nitrification, since it is an oxic process, and NH_4^+ effluxes from sediments suggested a consistent supply of substrate (Tables 5, 6; Figure 5). Nitrate flux was higher in A versus C cores in all incubations (Wilcoxon Signed-Rank, $p < 0.05$),

suggesting that, under normal conditions, nitrifiers were limited by NH_4^+ and stimulated by excess $^{15}NH_4^+$. Nitrate influxes observed when excess $^{15}NO_3^-$ was added (N cores) showed that NO_3^- in the settling pond was insufficient for denitrification to continuously exceed N fixation under *in situ* conditions. Net N fixation has been observed in stormwater wet ponds (Gold et al., in revision) and shallow, eutrophic flood control impoundments (Grantz et al., 2012) with low ambient NO_3^- concentrations. These results suggest the nitrifiers and denitrifiers were limited by N substrates in settling pond sediments under *in situ* conditions.

Nitrite was also released from pond sediments into overlying water in all treatments (C, A, N), indicating incomplete N transformations during the incubations (Figure 8). Nitrite is an intermediate of denitrification, nitrification, and DNRA, and net effluxes observed suggested that one or any of these processes did not proceed to completion (Lomas & Lipschultz, 2006). Nitrite efflux in C cores increased on May 26, 2020 (following fertilizer application), which was also when NH_4^+ and NO_3^- effluxes increased. These effluxes support the idea that excess NH_4^+ from the fertilizer application stimulated nitrification in sediments. In addition, net denitrification was observed during this incubation, so stimulation of nitrification provided substrate for denitrification. Furthermore, increased NO_2^- and NH_4^+ effluxes may have stimulated anammox, as its contribution to N_2 removal peaked during this incubation.

Nitrite fluxes in A and N cores can indicate incomplete nitrification and denitrification, respectively. In winter through early spring, NO_2^- effluxes were higher in A versus C cores (Wilcoxon Sign-Test, $p < 0.05$), suggesting that nitrification was the primary N transformation occurring, while NO_2^- effluxes in N cores were generally

higher than in C cores during the summer, suggesting primarily denitrification. Nitrification uses inorganic carbon as an electron donor, while denitrification uses organic carbon (Burgin & Hamilton, 2007; Guisasola et al., 2007). Thus, nitrification would be the expected major pathway during winter, after the most labile organic matter from the growing season was already remineralized, while denitrification would be the expected primary pathway during summer, when fresh organic matter was plentiful. Low concentrations in the pond suggest that NO_2^- is fully transformed at some point. Nitrite is also toxic to many microbes, so it is often transformed quickly by denitrification, nitrification, or DNRA (Glass & Silverstein, 1998). Jayakumar et al. (2009) found temporal differences in N forms during different stages of denitrification in oxygen minimum zones. As denitrification progresses and conditions shift from oxic to suboxic, denitrifier activity increases, and NO_2^- accumulates during intermediate stages until complete anoxia was reached, and then all oxidized forms are reduced to N_2.

SRP was released from sediments into the overlying water during all incubations (except July 1, 2020; Figure 6). SRP can be released as organic matter is decomposed and can then be assimilated by phytoplankton (Ward et al., 2009). Low SRP fluxes and ambient concentrations are likely the result of rapid uptake by phytoplankton and macrophytes (Table 8, Figure 6). A slight increase in SRP efflux was observed on May 26, 2020 (following fertilizer application; 24% P). However, SRP effluxes remained low (0.444 μmol P m^{-2} h^{-1}) compared to effluxes in studies of eutrophic systems, such as Lake Erie (range: 0.06 – 13 μmol P m^{-2} h^{-1}; Boedecker et al., 2020), Old Woman Creek (1.4 – 16.6 μmol P m^{-2} h^{-1}; McCarthy et al., 2007), and Florida Bay (range: 0.1 – 13 μmol P m^{-2} h^{-1}; Gardner and McCarthy, 2009). Low SRP effluxes in this study may be explained by

no applications of P-containing fertilizer or by rapid uptake by crops before SRP reached the pond or the phytoplankton/macrophyte community in the pond.

In winter and early spring, SRP fluxes in A cores were lower than in C cores, and net SRP uptake was observed in A cores. Likewise, in summer, SRP fluxes in N cores were lower than in C cores. This pattern suggests that the sediment microbial community may use excess N to better access or assimilate SRP (possibly through alkaline phosphatase; Cotner & Wetzel, 1991; Dyhrman & Ruttenberg, 2006) and reinforces the need for managing P and N in concert (Hamilton et al. 2016).

Evaluation of Settling Pond for Nitrogen Removal

Although settling pond sediments were a source of N throughout most of the sampling period, these sediments exhibited a switch from net N fixation at most times to net denitrification following pulses of N loading. In all cases, N_2 production was stimulated by $^{15}NO_3^-$ additions. These results show that denitrification was NO_3^- limited, and that denitrifiers were capable of removing excess N loading from fertilizer application. Low N loads also limited denitrification rates in a small reservoir in central Wisconsin (Richardson & Herrman, 2020). Similar to the Fondriest settling pond, low ambient NO_3^- concentrations favored N fixation and limited denitrification rates in a stormwater wet pond, leading to less permanent N removal (Gold et al., in revision). Other studies have found that constructed ponds and agricultural reservoirs are overall N sinks and important additions to management strategies aimed at minimizing nutrient exports. However, these landscapes were characterized by consistently high N (David et al., 2006; Fleischer et al., 1994; Powers et al., 2015).

Total yearly N removal by sediments in the settling pond was estimated based on the best estimate of *in situ* denitrification rates (Figure 16). Total N removal through denitrification was estimated to be 28 kg N yr^{-1}, but the total N load to the Fondriest settling pond is unknown. The highest ambient NO_3^- concentration in the wetland (181 µM) followed a fertilizer application (Table 2), and potential denitrification in the settling pond was 100 µmol N m^{-2} h^{-1} at that time. Using the surface area of the pond (4,046 m^2), it was estimated that pond sediments could remove 181 µM N in 54 hours. Rapid N removal may help explain why low ambient N concentrations were observed at all sampling events, including May 26, 2020, four days after a fertilizer application. A critical knowledge gap identified from this study involves quantifying, at more frequent intervals or during rain events, how much N is added to the pond system through N fixation in sediments and the water column relative to permanent N removal via denitrification and the total N load to the pond. This knowledge would allow a better understanding of the N budget and the extent to which the settling pond is capable of mitigating excess N loading from the agricultural watershed.

Bioavailable N added to the overlying water from sediments was estimated based on net nutrient fluxes (DIN + urea) in unamended C cores at 33.0 kg N yr^{-1}. The greater amount of N added by sediments compared to removal through denitrification (28 kg N yr^{-1}) supports the conclusion that the settling pond was a net source of N for most of the year. Despite the net release of nutrients, ambient N concentrations in the settling pond remained BDL or low during all sampling events, which was likely due in part to uptake by submerged vegetation around the perimeter of the pond. However, when using net nutrient fluxes in N cores to estimate internal N loading during pulse N

loading conditions, pond sediments acted as a net N sink and removed 19.7 kg N yr^{-1}. Net denitrification observed following N fertilizer application, consistent potential denitrification rates in N cores, and low ambient NO_3^- concentrations in the settling pond compared to the wetland all suggest that the settling pond performs a valuable ecosystem service for this system via N removal. If N fertilizer was applied more frequently or in larger quantities, pond sediments may play an even more important role in N removal and mitigating excess N loading, while helping prevent these N loads from reaching river networks and vulnerable receiving waters.

Directions for Future Work

Results from this study showed that the Fondriest settling pond acted as an overall N source via net N fixation and organic matter remineralization. However, when an N load (fertilizer application) was applied, or a rain event occurred, pond sediments were able to rapidly remove the added N through denitrification and function better at permanent N removal than the wetland. These findings show that the settling pond was an important addition to the wetland in terms of agricultural runoff management, but there are still aspects to the microbial functioning of the settling pond that need to be better understood.

Rain events can be influential in providing increased N loads to water bodies (Poe et al., 2003; She et al., 2018). Sampling events during this study were not coordinated with expected rain events, so the impacts from these events were not specifically tested. However, net denitrification rates measured in September 2019 and May 2020 suggest that rain events may drive N loss through denitrification by adding N to the settling pond. Future work should coordinate monitoring and sampling with forecasted rain events to

help understand the dynamics of runoff from agricultural fields and the responses of the wetland and settling pond. For example, ambient nutrient and physicochemical data could be continuously collected from the wetland and settling pond before, during, and after a rain event. Sediment core incubations could also be conducted at these times to observe any changes in dissolved gas and nutrient fluxes. The results from these kinds of sampling regimes would provide insight into how quickly sediments react to pulses of N from rain events and determine to what extent rain events are an important source of N.

Results from this study also suggest that N availability was an important factor determining whether net N fixation or net denitrification occurred in pond sediments. The agricultural landscape of the settling pond was expected to be influential to N cycling in the pond due to high N loads (fertilizer applications) from the adjacent crop field. Future studies should investigate how pond sediments function in response to more frequent fertilizer applications to determine if the sediments remain capable of removing repeated N loads due to fertilizer application.

Nitrogen fixation was an important process in the settling pond, but ambient N concentrations remained low. Future work could evaluate the importance of adding fixed N to the system using $^{30}N_2$ incubation techniques. The rate of ^{15}N incorporation into biomass would offer a better understanding of how quickly fixed N becomes bioavailable in the settling pond and the magnitude of N fixation as a source of N. Newell et al. (2016) used $^{30}N_2$ amended sediment cores and $^{15}NH_4^+$ production to directly estimate N fixation in coastal estuary sediments. Direct estimates of N fixation were more accurate compared to calculated N fixation. The rate at which bioavailable fixed N reappears in the water column could offer insight into the relative importance of sediments as a net N source

between runoff events and better understand microbial activities occurring in agricultural settling ponds.

V. CONCLUSION

This study highlights the importance of microbial N transformations to nutrient and dissolved gas cycling in agricultural settling pond sediments. Overall, pond sediments acted as a net source of NH_4^+, NO_3^-, NO_2^-, SRP, and urea, which are bioavailable nutrient forms used by primary producers for biomass production, metabolism, and reproduction. Denitrification was the primary N removal mechanism, with anammox contributing up to 8% of total N_2 removal. DNRA was not detected in all sediment cores and contributed up to 7% of total NH_4^+ release from sediments. SOD and potential denitrification rates were higher in spring and summer, likely due to increased microbial activity and organic matter production.

Pond sediments permanently removed excess N via denitrification following fertilizer applications and rain-driven N pulses. The sediments switched from net N fixation to net denitrification following a rain event in September 2019 and an N fertilizer application in May 2020. Potential denitrification rates (N cores) exceeded best estimates of *in situ* denitrification and indicated that denitrifiers could remove a greater N load throughout the entire year. In addition, ambient nutrient concentrations in the settling pond were lower than those in the wetland, suggesting more rapid nutrient removal in the pond. Best estimates of *in situ* denitrification were positive during all incubations, which confirmed that sediments were constantly removing N throughout the entire sampling period, despite the opposite effects of net N fixation during most incubations.

Settling pond sediments were estimated to remove 28 kg N yr^{-1} during this study, but the total N load to the settling pond is not known. Pond sediments released 35 kg N yr^{-1} to the overlying water, so N removal through denitrification could not compensate for nutrients added by the sediments. However, under consistent N loading (N cores), pond sediments removed net 16.9 kg N yr^{-1}; thus, pond sediments can be more effective at N removal under higher N loading conditions. However, higher N loading decreases denitrification efficiency, allowing excess N to remain in the system (Gardner & McCarthy, 2009; Mulholland et al., 2008). It was estimated that pond sediments could denitrify a typical load of N (180 µM, maximum NO_3^- concentration measured in the wetland outflow) in 2.25 days (54 hours), which may explain why ambient N concentrations in the pond remained below 7.7 µM (DIN + urea) during each sampling event, even within four days after fertilizer application. The results from this study confirm that settling pond sediments were an important location of N removal, when N loads were applied, and thus are a useful addition to agricultural nutrient mitigation practices. The extent that the settling pond experiences N loadings and net denitrification, compared to net N fixation, throughout the year should be evaluated to understand if permanent N removal via denitrification can offset N added through N fixation and organic matter remineralization.

VI. REFERENCES

An, S., Gardner, W. S., & Kana, T. (2001). Simultaneous measurement of denitrification and nitrogen fixation using isotope pairing with membrane inlet mass spectrometry analysis. *Applied and environmental microbiology*, *67*(3), 1171-1178.

Berman, T., Béchemin, C., & Maestrini, S. Y. (1999). Release of ammonium and urea from dissolved organic nitrogen in aquatic ecosystems. *Aquatic Microbial Ecology*, *16*(3), 295-302.

Bingham, M., Sinha, S. K., & Lupi, F. (2015). Economic benefits of reducing harmful algal blooms in Lake Erie. *Environmental Consulting & Technology, Inc., Report*, *66*.

Boedecker, A. R., Niewinski, D. N., Newell, S. E., Chaffin, J. D., & McCarthy, M. J. (2020). Evaluating sediments as an ecosystem service in western Lake Erie via quantification of nutrient cycling pathways and selected gene abundances. *Journal of Great Lakes Research*, *46*(4), 920-932.

Bruesewitz, D. A., Hamilton, D. P., & Schipper, L. A. (2011). Denitrification potential in lake sediment increases across a gradient of catchment agriculture. *Ecosystems*, *14*(3), 341-352.

Burgin, A. J., & Hamilton, S. K. (2007). Have we overemphasized the role of denitrification in aquatic ecosystems? A review of nitrate removal pathways. *Frontiers in Ecology and the Environment*, *5*(2), 89-96.

Camargo Valero, M. A., Mara, D. D., & Newton, R. J. (2010). Nitrogen removal in maturation waste stabilisation ponds via biological uptake and sedimentation of dead biomass. *Water science and technology*, *61*(4), 1027-1034.

Camargo, J. A., & Alonso, Á. (2006). Ecological and toxicological effects of inorganic nitrogen pollution in aquatic ecosystems: a global assessment. *Environment international*, *32*(6), 831-849.

Chaffin, J. D., Bridgeman, T. B., Heckathorn, S. A., & Mishra, S. (2011). Assessment of Microcystis growth rate potential and nutrient status across a trophic gradient in western Lake Erie. *Journal of Great Lakes Research*, *37*(1), 92-100.

Clarkson, B. R., Ausseil, A. G. E., & Gerbeaux, P. (2013). Wetland ecosystem services. *Ecosystem services in New Zealand: conditions and trends. Manaaki Whenua Press, Lincoln*, 192-202.

Conley, D. J., Paerl, H. W., Howarth, R. W., Boesch, D. F., Seitzinger, S. P., Karl E, K. E., ... & Gene E, G. E. (2009). Controlling eutrophication: nitrogen and phosphorus. *Science*, *123*, 1014-1015.

Cotner, J. B., & Wetzel, R. G. (1991). 5′-Nucleotidase activity in a eutrophic lake and an oligotrophic lake. *Applied and environmental microbiology*, *57*(5), 1306-1312.

Craft, C. B. (1996). Dynamics of nitrogen and phosphorus retention during wetland ecosystem succession. *Wetlands Ecology and Management* 4.3: 177-187.

David, M. B., Wall, L. G., Royer, T. V., & Tank, J. L. (2006). Denitrification and the nitrogen budget of a reservoir in an agricultural landscape. *Ecological Applications*, *16*(6), 2177-2190.

Davidson, N. C. (2014). How much wetland has the world lost? Long-term and recent trends in global wetland area. *Marine and Freshwater Research*, *65*(10), 934-941.

Dodds, W. K., Bouska, W. W., Eitzmann, J. L., Pilger, T. J., Pitts, K. L., Riley, A. J., ... & Thornbrugh, D. J. (2009). Eutrophication of US freshwaters: analysis of potential economic damages.

Dyhrman, S. T., & Ruttenberg, K. C. (2006). Presence and regulation of alkaline phosphatase activity in eukaryotic phytoplankton from the coastal ocean: Implications for dissolved organic phosphorus remineralization. *Limnology and Oceanography*, *51*(3), 1381-1390.

Ferrara, R. A., & Avci, C. B. (1982). Nitrogen dynamics in waste stabilization ponds. *Journal (Water Pollution Control Federation)*, 361-369.

Fisher, J., & Acreman, M. C. (2004). Wetland nutrient removal: a review of the evidence. *Hydrology and Earth system sciences*, *8*(4), 673-685.

Fleischer, S., Gustafson, A., Joelsson, A., Pansar, J., & Stibe, L. (1994). Nitrogen removal in created ponds. *Ambio*, 349-357.

Fulweiler, R. W., Brown, S. M., Nixon, S. W., & Jenkins, B. D. (2013). Evidence and a conceptual model for the co-occurrence of nitrogen fixation and denitrification in heterotrophic marine sediments. *Marine Ecology Progress Series*, *482*, 57-68.

Gale, P. M., Devai, I., Reddy, K. R., & Graetz, D. A. (1993). Denitrification potential of soils from constructed and natural wetlands. *Ecological Engineering*, *2*(2), 119-130.

Galloway, J. N. (1998). The global nitrogen cycle: changes and consequences. *Environmental pollution*, *102*(1), 15-24.

Galloway, J. N., & Cowling, E. B. (2002). Reactive nitrogen and the world: 200 years of change. *AMBIO: A Journal of the Human Environment*, *31*(2), 64-71.

Gardner, W. S., & McCarthy, M. J. (2009). Nitrogen dynamics at the sediment–water interface in shallow, sub-tropical Florida Bay: why denitrification efficiency may decrease with increased eutrophication. *Biogeochemistry*, *95*(2), 185-198.

Gardner, W. S., McCarthy, M. J., An, S., Sobolev, D., Sell, K. S., & Brock, D. (2006). Nitrogen fixation and dissimilatory nitrate reduction to ammonium (DNRA) support nitrogen dynamics in Texas estuaries. *Limnology and Oceanography*, *51*(1part2), 558-568.

Glass, C., & Silverstein, J. (1998). Denitrification kinetics of high nitrate concentration water: pH effect on inhibition and nitrite accumulation. *Water Research*, *32*(3), 831-839.

Gold, A. C., Thompson, S. P., & Piehler, M. F. (in revision at Water Resources Research). Impacts of temperature and precipation on the fate of nitrogen in coastal stormwater wet ponds.

Gopal, B. (1999). Natural and constructed wetlands for wastewater treatment: potentials and problems. *Water science and technology*, *40*(3), 27-35.

Grantz, E. M., Kogo, A., & Scott, J. T. (2012). Partitioning whole-lake denitrification using in situ dinitrogen gas accumulation and intact sediment core experiments. *Limnology and oceanography*, *57*(4), 925-935.

Groh, T. A., Gentry, L. E., & David, M. B. (2015). Nitrogen removal and greenhouse gas emissions from constructed wetlands receiving tile drainage water. *Journal of environmental quality*, *44*(3), 1001-1010.

Guisasola, A., Petzet, S., Baeza, J. A., Carrera, J., & Lafuente, J. (2007). Inorganic carbon limitations on nitrification: experimental assessment and modelling. *Water research*, *41*(2), 277-286.

Gupta, C., Prakash, D., & Gupta, S. (2015). Role of blue green algae in environment management. *Environmental Microbiology. IK International Publishing House Pvt. Ltd., India*.

Halide, H., Ridd, P. V., Peterson, E. L., & Foster, D. (2003). Assessing sediment removal capacity of vegetated and non-vegetated settling ponds in prawn farms. *Aquacultural engineering*, *27*(4), 295-314.

Hamilton, D. P., Salmaso, N., & Paerl, H. W. (2016). Mitigating harmful cyanobacterial blooms: strategies for control of nitrogen and phosphorus loads. *Aquatic Ecology*, *50*(3), 351-366.

Healy, M., & Cawley, A. M. (2002). Nutrient processing capacity of a constructed wetland in western Ireland. *Journal of Environmental Quality*, *31*(5), 1739-1747.

Herbert, R. A. (1975). Heterotrophic nitrogen fixation in shallow estuarine sediments. *Journal of Experimental Marine Biology and Ecology*, *18*(3), 215-225.

Hernandez, M. E., & Mitsch, W. J. (2007). Denitrification potential and organic matter as affected by vegetation community, wetland age, and plant introduction in created wetlands. *Journal of environmental quality*, *36*(1), 333-342.

Howarth, R. W., Marino, R., & Cole, J. J. (1988). Nitrogen fixation in freshwater, estuarine, and marine ecosystems. 2. Biogeochemical controls. *Limnology and Oceanography*, *33*(4), 688-701.

Huang, J., Cai, W., Zhong, Q., & Wang, S. (2013). Influence of temperature on micro-environment, plant eco-physiology and nitrogen removal effect in subsurface flow constructed wetland. *Ecological Engineering*, *60*, 242-248.

Ilyas, H., & Masih, I. (2017). The performance of the intensified constructed wetlands for organic matter and nitrogen removal: A review. *Journal of environmental management*, *198*, 372-383.

Jackson, C. J., Preston, N., Burford, M. A., & Thompson, P. J. (2003). Managing the development of sustainable shrimp farming in Australia: the role of sedimentation ponds in treatment of farm discharge water. *Aquaculture*, *226*(1-4), 23-34.

Jansson, M., Andersson, R., Berggren, H., & Leonardson, L. (1994). Wetlands and lakes as nitrogen traps. *Ambio*, 320-325.

Jayakumar, A., O'Mullan, G. D., Naqvi, S. W. A., & Ward, B. B. (2009). Denitrifying bacterial community composition changes associated with stages of denitrification in oxygen minimum zones. *Microbial ecology*, *58*(2), 350-362.

Jenkins, M. C., & Kemp, W. M. (1984). The coupling of nitrification and denitrification in two estuarine sediments 1, 2. *Limnology and Oceanography*, *29*(3), 609-619.

Jiang, X., Gao, G., Zhang, L., Tang, X., Shao, K., & Hu, Y. (2020). Denitrification and dissimilatory nitrate reduction to ammonium in freshwater lakes of the Eastern Plain, China: influences of organic carbon and algal bloom. *Science of The Total Environment*, *710*, 136303.

Jordan, S. J., Stoffer, J., & Nestlerode, J. A. (2011). Wetlands as sinks for reactive nitrogen at continental and global scales: a meta-analysis. *Ecosystems*, *14*(1), 144-155.

Kana, T. M., Darkangelo, C., Hunt, M. D., Oldham, J. B., Bennett, G. E., & Cornwell, J. C. (1994). Membrane inlet mass spectrometer for rapid high-precision determination of N2, O2, and Ar in environmental water samples. *Analytical Chemistry*, *66*(23), 4166-4170.

Keffala, C., Galleguillos, M., Ghrabi, A., & Vasel, J. L. (2011). Investigation of nitrification and denitrification in the sediment of wastewater stabilization ponds. *Water, Air, & Soil Pollution*, *219*(1), 389-399.

Kuenen, J. G. (2008). Anammox bacteria: from discovery to application. *Nature Reviews Microbiology*, *6*(4), 320-326.

Kuschk, P., Wiessner, A., Kappelmeyer, U., Weissbrodt, E., Kästner, M., & Stottmeister, U. (2003). Annual cycle of nitrogen removal by a pilot-scale subsurface horizontal flow in a constructed wetland under moderate climate. *Water Research*, *37*(17), 4236-4242.

Lavrentyev, P. J., Gardner, W. S., & Yang, L. (2000). Effects of the zebra mussel on nitrogen dynamics and the microbial community at the sediment-water interface. *Aquatic Microbial Ecology*, *21*(2), 187-194.

Lee, C. G., Fletcher, T. D., & Sun, G. (2009). Nitrogen removal in constructed wetland systems. *Engineering in Life Sciences*, *9*(1), 11-22.

Li, F., Yang, R., Ti, C., Lang, M., Kimura, S. D., & Yan, X. (2010). Denitrification characteristics of pond sediments in a Chinese agricultural watershed. *Soil Science & Plant Nutrition*, *56*(1), 66-71.

Lomas, M. W., & Lipschultz, F. (2006). Forming the primary nitrite maximum: nitrifiers or phytoplankton?. *Limnology and Oceanography*, *51*(5), 2453-2467.

Lu, S., Zhang, P., Jin, X., Xiang, C., Gui, M., Zhang, J., & Li, F. (2009). Nitrogen removal from agricultural runoff by full-scale constructed wetland in China. *Hydrobiologia*, *621*(1), 115-126.

Mayo, A. W., & Abbas, M. (2014). Removal mechanisms of nitrogen in waste stabilization ponds. *Physics and Chemistry of the Earth, Parts A/B/C*, *72*, 77-82.

McCarthy, M. J., Gardner, W. S., Lavrentyev, P. J., Moats, K. M., Jochem, F. J., & Klarer, D. M. (2007). Effects of hydrological flow regime on sediment-water interface and water column nitrogen dynamics in a Great Lakes coastal wetland (Old Woman Creek, Lake Erie). *Journal of Great Lakes Research*, *33*(1), 219-231.

McCarthy, M. J., Gardner, W. S., Lehmann, M. F., Guindon, A., & Bird, D. F. (2016). Benthic nitrogen regeneration, fixation, and denitrification in a temperate, eutrophic lake: Effects on the nitrogen budget and cyanobacteria blooms. *Limnology and Oceanography*, *61*(4), 1406-1423.

McCarthy, M. J., Newell, S. E., Carini, S. A., & Gardner, W. S. (2015). Denitrification dominates sediment nitrogen removal and is enhanced by bottom-water hypoxia in the Northern Gulf of Mexico. *Estuaries and Coasts*, *38*(6), 2279-2294.

Mietto, A., Politeo, M., Breschigliaro, S., & Borin, M. (2015). Temperature influence on nitrogen removal in a hybrid constructed wetland system in Northern Italy. *Ecological Engineering*, *75*, 291-302.

Morris, J. T. (1991). Effects of nitrogen loading on wetland ecosystems with particular reference to atmospheric deposition. *Annual Review of Ecology and Systematics*, *22*(1), 257-279.

Mulholland, P. J., Helton, A. M., Poole, G. C., Hall, R. O., Hamilton, S. K., Peterson, B. J., Tank, J. L, Ashkenas, L. R., Cooper, L. W., Dahm, C. N., Dodds, W. K., Findlay, S. E. G., Gregory, S. V., Grimm, N. B., Johnson, S. L., McDowell, W. H., Meyer, J. L., Valett, H. M., Webster, J. R., Arango, C. P., Beaulieu, J. J., Bernot, M. J., Burgin, A. J., Crenshaw, C. L., Johnson, L. T., Niederlehner, B. R., O'Brien, J. M., Potter, J. D., Sheiblery, R. W., Sobota, D. J., & Thomas, S. M. (2008). Stream denitrification across biomes and its response to anthropogenic nitrate loading. *Nature*, *452*(7184), 202-205.

Newell, S. E., McCarthy, M. J., Gardner, W. S., & Fulweiler, R. W. (2016). Sediment nitrogen fixation: a call for re-evaluating coastal N budgets. *Estuaries and Coasts*, *39*(6), 1626-1638.

Nichols, D. S. (1983). Capacity of natural wetlands to remove nutrients from wastewater. *Journal (Water Pollution Control Federation)*, 495-505.

Paerl, H. (2008). Nutrient and other environmental controls of harmful cyanobacterial blooms along the freshwater–marine continuum. In *Cyanobacterial harmful algal blooms: State of the science and research needs* (pp. 217-237). Springer, New York, NY.

Paerl, H. W., & Otten, T. G. (2013). Harmful cyanobacterial blooms: causes, consequences, and controls. *Microbial ecology*, *65*(4), 995-1010.

Poe, A. C., Piehler, M. F., Thompson, S. P., & Paerl, H. W. (2003). Denitrification in a constructed wetland receiving agricultural runoff. *Wetlands*, *23*(4), 817-826.

Powers, S. M., Tank, J. L., & Robertson, D. M. (2015). Control of nitrogen and phosphorus transport by reservoirs in agricultural landscapes. *Biogeochemistry*, *124*(1), 417-439.

Rahman, M. M., Roberts, K. L., Warry, F., Grace, M. R., & Cook, P. L. (2019). Factors controlling dissimilatory nitrate reduction processes in constructed stormwater urban wetlands. *Biogeochemistry*, *142*(3), 375-393.

Reed, S. C. (1985). Nitrogen removal in wastewater stabilization ponds. *Journal (Water Pollution Control Federation)*, 39-45.

Reinhardt, M., Müller, B., Gächter, R., & Wehrli, B. (2006). Nitrogen removal in a small constructed wetland: an isotope mass balance approach. *Environmental science & technology*, *40*(10), 3313-3319.

Richardson, B. L., & Herrman, K. S. (2020). Nitrogen Removal via Denitrification in Two Small Reservoirs in Central Wisconsin, USA. *The American Midland Naturalist*, *184*(1), 73-86.

Schubert, C. J., Durisch-Kaiser, E., Wehrli, B., Thamdrup, B., Lam, P., & Kuypers, M. M. (2006). Anaerobic ammonium oxidation in a tropical freshwater system (Lake Tanganyika). *Environmental microbiology*, *8*(10), 1857-1863.

Scott, J. T., McCarthy, M. J., Gardner, W. S., & Doyle, R. D. (2008). Denitrification, dissimilatory nitrate reduction to ammonium, and nitrogen fixation along a nitrate concentration gradient in a created freshwater wetland. *Biogeochemistry*, *87*(1), 99-111.

Seiki, T., Izawa, H., Date, E., & Sunahara, H. (1994). Sediment oxygen demand in Hiroshima Bay. *Water Research*, *28*(2), 385-393.

Seitzinger, S. (2008). Out of reach. *Nature*, *452*(7184), 162-163.

Seitzinger, S. P. (1988). Denitrification in freshwater and coastal marine ecosystems: ecological and geochemical significance. *Limnology and oceanography*, *33*(4part2), 702-724.

Senzia, M. A., Mayo, A. W., Mbwette, T. S. A., Katima, J. H. Y., & Jørgensen, S. E. (2002). Modelling nitrogen transformation and removal in primary facultative ponds. *Ecological Modelling*, *154*(3), 207-215.

She, D., Zhang, L., Gao, X., Yan, X., Zhao, X., Xie, W., Cheng, Y., & Xia, Y. (2018). Limited N removal by denitrification in agricultural drainage ditches in the Taihu Lake region of China. *Journal of soils and sediments*, *18*(3), 1110-1119.

Shen, L. D., Cheng, H. X., Liu, X., Li, J. H., & Liu, Y. (2017). Potential role of anammox in nitrogen removal in a freshwater reservoir, Jiulonghu Reservoir (China). *Environmental Science and Pollution Research*, *24*(4), 3890-3899.

Smith, V. H., Tilman, G. D., & Nekola, J. C. (1999). Eutrophication: impacts of excess nutrient inputs on freshwater, marine, and terrestrial ecosystems. *Environmental pollution*, *100*(1-3), 179-196.

Steffen, M. M., Davis, T. W., McKay, R. M. L., Bullerjahn, G. S., Krausfeldt, L. E., Stough, J. M., Neitzey, M. L., Gilbert, N. E., Boyer, G. L., Johengen, T. H., Gossiaux, D. C., Burtner, A. M., Palladino, D., Rowe, M. D., Dick, G. J., Meyer, K. A., Levy, S., Boone, B. E., Stumpf, R. P., Wynne, T. T., Zimba, P. V., Gutierrez, D., & Wilhelm, S. W. (2017). Ecophysiological examination of the Lake Erie Microcystis bloom in 2014: linkages between biology and the water supply shutdown of Toledo, OH. *Environmental science & technology*, *51*(12), 6745-6755.

Sutula, M., Kudela, R., Hagy III, J. D., Harding Jr, L. W., Senn, D., Cloern, J. E., Bricker, S., Berg, G. M., & Beck, M. (2017). Novel analyses of long-term data provide a scientific basis for chlorophyll-a thresholds in San Francisco Bay. *Estuarine, coastal and shelf science*, *197*, 107-118.

Teichert-Coddington, D. R., Rouse, D. B., Potts, A., & Boyd, C. E. (1999). Treatment of harvest discharge from intensive shrimp ponds by settling. *Aquacultural Engineering*, *19*(3), 147-161.

Tournebize, J., Chaumont, C., Fesneau, C., Guenne, A., Vincent, B., Garnier, J., & Mander, Ü. (2015). Long-term nitrate removal in a buffering pond-reservoir system receiving water from an agricultural drained catchment. *Ecological Engineering*, *80*, 32-45.

Uusheimo, S., Huotari, J., Tulonen, T., Aalto, S. L., Rissanen, A. J., & Arvola, L. (2018a). High nitrogen removal in a constructed wetland receiving treated wastewater in a cold climate. *Environmental science & technology*, *52*(22), 13343-13350.

Uusheimo, S., Tulonen, T., Aalto, S. L., & Arvola, L. (2018b). Mitigating agricultural nitrogen load with constructed ponds in northern latitudes: A field study on sedimental denitrification rates. *Agriculture, Ecosystems & Environment, 261*, 71-79.

Vitousek, P. M., Menge, D. N., Reed, S. C., & Cleveland, C. C. (2013). Biological nitrogen fixation: rates, patterns and ecological controls in terrestrial ecosystems. *Philosophical Transactions of the Royal Society B: Biological Sciences, 368*(1621), 20130119.

Vymazal, J. (2007). Removal of nutrients in various types of constructed wetlands. *Science of the total environment, 380*(1-3), 48-65.

Ward, B. B., Devol, A. H., Rich, J. J., Chang, B. X., Bulow, S. E., Naik, H., Pratihary, A., & Jayakumar, A. (2009). Denitrification as the dominant nitrogen loss process in the Arabian Sea. *Nature, 461*(7260), 78-81.

Washbourne, I. J., Crenshaw, C. L., & Baker, M. A. (2011). Dissimilatory nitrate reduction pathways in an oligotrophic freshwater ecosystem: spatial and temporal trends. *Aquatic microbial ecology, 65*(1), 55-64.

Wenk, C. B., Blees, J., Zopfi, J., Veronesi, M., Bourbonnais, A., Schubert, C. J., Niemann, H., & Lehmann, M. F. (2013). Anaerobic ammonium oxidation (anammox) bacteria and sulfide-dependent denitrifiers coexist in the water column of a meromictic south-alpine lake. *Limnology and Oceanography, 58*(1), 1-12.

Wituszynski, D. M., Hu, C., Zhang, F., Chaffin, J. D., Lee, J., Ludsin, S. A., & Martin, J. F. (2017). Microcystin in Lake Erie fish: risk to human health and relationship to cyanobacterial blooms. *Journal of Great Lakes Research, 43*(6), 1084-1090.

Yin, G., Hou, L., Liu, M., Liu, Z., & Gardner, W. S. (2014). A novel membrane inlet mass spectrometer method to measure 15NH4+ for isotope-enrichment experiments in aquatic ecosystems. *Environmental science & technology*, *48*(16), 9555-9562.

Zak, D., Kronvang, B., Carstensen, M. V., Hoffmann, C. C., Kjeldgaard, A., Larsen, S. E., Audet, J., Egemose, S., Jorgensen, C. A., Feuerbach, P., Gertz, F., & Jensen, H. S. (2018). Nitrogen and phosphorus removal from agricultural runoff in integrated buffer zones. *Environmental science & technology*, *52*(11), 6508-6517.

Zhao, Y., Xia, Y., Kana, T. M., Wu, Y., Li, X., & Yan, X. (2013). Seasonal variation and controlling factors of anaerobic ammonium oxidation in freshwater river sediments in the Taihu Lake region of China. *Chemosphere*, *93*(9), 2124-213